

SG-112-6

TWO-PHASE FLOW IN GEOTHERMAL WELLS:
DEVELOPMENT AND USES OF A COMPUTER CODE

A Report

Submitted to the Department of Petroleum Engineering
of Stanford University
in partial fulfillment of the requirements
for the degree of

MASTER OF SCIENCE

by

Jaime Ortiz-Ramirez

June 1983

ACKNOWLEDGEMENT

I would like to thank Comision Federal de Electricidad de Mexico for financial support for my studies at Stanford University. I greatly appreciate the additional support received from the Stanford Geothermal Program.

I appreciate the help given by the Instituto de Investigaciones Electricas de Mexico in obtaining the Cerro Prieto Data.

I am in a great debt with Prof. Jon S. Gudmundsson for his suggestions and effort as my research advisor.

I want to thank Prof. Roland N. Horne for his advise during my studies at Stanford.

Finally, I want to express my thanks to my wife for her patience and encouragement during my graduate studies.

ABSTRACT

A computer code is developed for vertical two-phase flow in geothermal wellbores. The two-phase correlations used were developed by Orkiszewski (1967) and others and are widely applicable in the oil and gas industry.

The computer code is compared to the flowing survey measurements from wells in the East Mesa, Cerro Prieto, and Roosevelt Hot Spring geothermal fields with success. Well data from the Svartsengi field in Iceland are also used.

Several applications of the computer code are considered. They range from reservoir analysis to wellbore deposition studies. It is considered that accurate and workable wellbore simulators have an important role to play in geothermal reservoir engineering.

TABLE OF CONTENTS

	Page
ABSTRACT	
1. INTRODUCTION	1
2. LITERATURE SURVEY	3
3. VERTICAL TWO-PHASE FLOW	
3.1 Description	6
3.2 Two-Phase Flow Equations	9
3.3 Two-Phase Flow Correlations	11
3.4 Single-Phase Liquid Flow	17
3.5 Heat Transfer Equations	18
4. COMPUTER CODE	
4.1 Description	20
4.2 Validation	24
5. USES OF WELLBORE MODELS	
5.1 Pressure and Temperature Profiles	28
5.2 Discharge Analysis	29
5.3 Casing Design	31
5.4 Fluid Enthalpy	33

5.5 Scale Deposition	34
5.6 Wellbore Heat Transfer	36
5.7 Well Test Analysis	37
5.8 Decline Curves	38
6. CONCLUSIONS	39
NOMENCLATURE	41
REFERENCES	
APPENDIX A Flow Diagram and Program Listing	
APPENDIX B Data Used	
APPENDIX C Derivation of equations	

1. INTRODUCTION

In geothermal field development the engineer is concerned with fluid flow in the reservoir and wellbore. Two-phase flow occurs in the wellbore of the wells in liquid dominated reservoirs. The engineer is therefore interested in simulating two-phase wellbore flow to obtain information about the reservoir and production characteristics of wells.

Two-phase vertical flow in geothermal wells has been studied by many investigators. The equations that describe such flow are the continuity, momentum, and energy equations. These are then used to express the total pressure drop up the wellbore in terms of its potential, acceleration, and frictional components. In studies of this nature we are able to draw upon the extensive two-phase literature of the nuclear and oil and gas industries.

While many papers have been published with geothermal wellbore flow models, there are not many studies that show how these models can be used. The step from theoretical models to engineering applications seems not to have received a lot of attention. There may exist many applications which still need to be discovered. The problem

is that we do not have extensive measurements of geothermal well behavior. However, as more data becomes available it is important to have an accurate and workable wellbore simulator. Continuous interaction between field measurements and flow modeling studies should advance our understanding of geothermal well characteristics.

The main purpose of the present work was to develop a workable geothermal wellbore simulator, the work is based on earlier efforts at Stanford University. A new computer code was written with minor modifications of the commonly used two-phase flow correlations. The applications considered (8 main categories) are based on known problems in geothermal reservoir engineering.

2. LITERATURE SURVEY

Most of the available correlations^{1,3,4,5,7,9} for vertical two-phase flow in wells have been developed for the oil and gas industry. These correlations have been modified to suit the condition that exist in geothermal wells. A complete analytical description of one dimensional two-phase flow is given by Wallis⁸.

Gould⁶ used a combination of correlations from Hagedorn-Brown, Ros, Turner-Ros, Aziz, and Orkiszewski and coupled them with heat transfer equations to model two-phase flow in geothermal wellbores. The data he used to validate the model came from the Wairakei and Broadlands geothermal fields in New Zealand and East Mesa in the Imperial Valley. Gould found that the Hagedorn-Brown and Turner-Ros correlations were the most consistent.

Upadhyay et al¹⁰ concluded that the correlations used by Orkiszewski¹ and Hagedorn-Brown⁴ predict accurately the overall pressure drop in geothermal wellbores. Fandriana et al² compared four different correlations and found that Orkiszewski gave the best result.

Chierici et al¹⁸ developed a geothermal wellbore model based on a previous work done by Chierici for oil and gas wells. They use the same criteria as Orkiszewski to determine the flow regimes. Barelli et al²² included the effect of non-condensable gases on wellbore flow. They varied CO₂ content to match the flowing temperature and pressure profiles. It was found that an increased CO₂ concentration brings about an increase in pressure but has little effect on temperature.

Nathenson⁴⁴ made calculations for a typical geothermal well showing the effects on production of varying reservoir parameters. Elliot¹² compared the available power at wellhead for self flowing and pumping wells. Butz and Plooster¹³ used a two-phase wellbore simulator to investigate the effects of well casing diameter and productivity index on the flowrate to show that casing design can be optimized.

Bilicki et al¹⁴ examined the effects of fluid temperature, pressure, equivalent salinity, reservoir drawdown coefficient, heat loss, and well They found that the most important parameter governing flow in geothermal wells is the reservoir temperature.

Miller¹⁵ has developed a wellbore model and coupled it with a simple reservoir model. The transient behavior of single and two-phase flow well during a well test was investigated. Hoang¹⁶ has also coupled reservoir and

wellbore models and reported good agreement with the reservoir properties calculated using conventional well testing techniques.

Goyal et al²⁴ used flowing surveys (temperature and pressure) from Cerro Prieto wells to compare with calculated pressure and temperature profiles. They found that the calculated profiles were quite sensitive to measured wellhead parameters and well inside diameter.

3. VERTICAL TWO-PHASE FLOW

3.1 Description

Vertical two-phase flow has mainly been studied by semi-empirical methods. Correlations that were developed for two-phase flow in oil and gas wells have successfully been applied to geothermal wells.

Orkiszewski¹ classified existing correlations for vertical two-phase flow in wells into three categories:

First, liquid holdup is not considered in the determination of the mixture density which is just corrected by pressure and temperature. Liquid holdup and the pressure losses are expressed using empirically correlated friction factor. There is not distinction between flow regimes.

Second, liquid holdup is considered in the calculation of mixture density. Holdup is correlated separately or in combination with friction losses. The friction losses are based on the properties of the mixture. There is not distinction between flow regimes.

Third, liquid holdup is used to calculate the mixture density. Holdup determination is based on the slip velocity

(difference between gas and liquid velocities). The friction losses are determined using the continuous phase. Four flow regimes are considered.

Hagedorn-Brown⁴ belongs to the second category, while the Duns-Ros³, and the Orkiszewski¹ correlations belong to the third category.

Flow regimes commonly used in the two-phase literature are as follow:

Bubble. In this regime the liquid phase is the continuous phase and occupies most of the pipe volume, and the gaseous phase appears as small bubbles distributed through the liquid. The liquid phase is decisive in the pressure gradient calculation.

Slug. The liquid phase remains as the continuous phase, but the bubbles have increased in number and size and now join to form a single bubble which form and size approaches the pipe diameter. The velocity this bubble is by far larger than the velocity of the liquid. Both liquid and gas contribute in the total pressure gradient.

Transition. In this regime the gaseous phase becomes the continuous phase and some liquid is entrained as small droplets into the gaseous phase. The gas has a greater influence on the total pressure gradient than the liquid.

Mist. The gaseous phase is the continuous phase and the

liquid is entrained in the gas. The gaseous phase controls the pressure gradient and liquid causes secondary effects.

when dealing with two-phase flow we have to refer to the saturation states of water. These are defined as states at which a phase change begins or ends¹⁷. The saturated-liquid line is the state at which the first bubble of steam forms, and the saturated-gas line is the state at which the first liquid droplet forms. The subscript "f" is commonly used to indicate states in the saturated-liquid line, and the states in the saturated-gas line will be referred by the subscript "g" .

If the quality x is defined as the fraction of the total mass which is saturated gas, enthalpy of the liquid-gas mixture h_m can be calculated from

$$h_m = (1 - x) h_f + x h_g \quad (1)$$

and specific volume of the gas-liquid mixture v_m will then be expressed by

$$v_m = (1 - x) v_f + x v_g \quad (2)$$

If the void fraction α also called gas holdup is the volume of gas or steam actually present in a given pipe section, expressed as the fraction of the total volume of

that pipe section, then the density of the liquid-gas mixture as a function of the void fraction is given by

$$\rho_m = (1 - \alpha) \rho_f + \alpha \rho_g \quad (3)$$

The superficial velocities V_{SL} and V_{SG} of liquid and gas respectively will be defined as

$$V_{SL} = q_L / A \quad (3a)$$

and

$$V_{SG} = q_g / A \quad (3b)$$

where q_L and q_g are the volumetric flowrates of the two phases and A is the cross-sectional flow area. Eqs. (1), (2), and (3) are derived in Appendix C.

3.2 Two-Phase Flow Equations

The basic equations for steady one-dimensional two-phase flow are, the continuity equation:

$$Wt = \rho_m V_m A \quad (4)$$

and the momentum equation

$$Wt \frac{dV_m}{dz} = - \frac{dp}{dz} A - \pi \tau_w D - \rho_m g A \quad (5)$$

Substituting Eq.(4) in Eq.(5) we get

$$\rho_m A V_m \frac{dV_m}{dz} = - \frac{dp}{dz} A - \pi \tau_w D - \rho_m g A \quad (6)$$

Multiplying the whole equation by dz/A and solving for $-dp$

$$-dp = \rho_m g dz + \pi \tau_w D \frac{dz}{A} + \rho_m V_m dV_m \quad (7)$$

$\left[\begin{array}{c} \text{Potential} \\ \text{Term} \end{array} \right]$

$\left[\begin{array}{c} \text{Friction} \\ \text{Term} \end{array} \right]$

$\left[\begin{array}{c} \text{Kinetic} \\ \text{Term} \end{array} \right]$

Rewriting the kinetic term of Eq.(7) as done by Poettmann and Carpenter

$$\rho_m V_m dV_m = - \frac{q_g Wt}{A^2 \bar{p}} dp \quad (8)$$

and denoting $\pi \tau_w D / A$ by t_f which is the pressure drop per unit length due to friction, Eq.(7) can be rewritten as

$$-dp = \rho_m g dz + t_f dz - \frac{q_g Wt}{A^2 \bar{p}} dp dz$$

Solving for $-dp$

$$-dp = \left[\frac{\rho_m g + t_f}{1 - \frac{q_g Wt}{A^2 \bar{p}}} \right] dz \quad (9)$$

The minus sign is needed because we are considering z as positive in the upward direction.

3.3 Two-Phase Flow Correlations

The procedure described by Orkiszewski¹ will be followed in this work. It has been used successfully in the oil and gas industry. Orkiszewski method has also been applied to geothermal wells giving reasonable results in determination of pressure drops. The method will now be described.

The flow regimes are determined as by Duns and Ros³. The upper limit for bubble flow in their pattern map was approximated by a third degree polynomial. In order to make use of this flow pattern map we need to get the liquid number N_L and the gas number N_g . For the units given in the nomenclature :

$$N_L = 1.938 V_{sL} (\rho_L / \sigma)^{1/4} \quad (10)$$

$$N_g = 1.938 V_{sg} (\rho_L / \sigma)^{1/4} \quad (11)$$

where σ is the surface tension (dynes/cm) , then the flow regimes are determined as follows :

$$\text{Bubble} \quad 0.1 < N_g < 1.024 + 1.475 N_L - 1.75 \times 10^{-2} N_L^2 + 1.088 \times 10^{-3} N_L^3 \quad (12)$$

$$\text{Slug} \quad N_g < 50 + 36 N_L \quad (13)$$

$$\text{Transition} \quad N_g < 75 + 84 N_L \quad (14)$$

$$\text{Mist} \quad N_g > 75 + 84 N_L \quad (15)$$

Once the flow regime is determined the value for ρ_m and t_f are obtained according to the following criteria.

Bubble flow

The density of the mixture ρ_m can be determined using Eq.(3)

$$\rho_m = (1 - \alpha) \rho_L + \alpha \rho_g \quad (3)$$

Where α is determined according to Griffith and Wallis⁹

$$\alpha = \frac{1}{2} \left[1 + \frac{q_t}{V_s A} - \sqrt{\left(1 + \frac{q_t}{V_s A} \right)^2 - \frac{4 q_g}{V_s A}} \right] \quad (16)$$

where V_s is the slip velocity and for which they suggested a value of 0.8 ft/sec .

The friction loss gradient t_f is given by

$$t_f = f \frac{V_L^2 \rho_L}{2 g D} \quad (17)$$

where V_L is the real velocity of liquid and is calculated as

$$V_L = \frac{q_L}{A (1 - \alpha)} \quad (18)$$

The friction factor f is obtained using a standard Moody diagram as a function of Reynolds number

$$N_{RE} = 1488 D V_L \rho_L / \mu_L \quad (19)$$

Slug flow

The density of the mixture ρ_m is calculated by

$$\rho_m = \frac{Wt + \rho_L Vb A}{q_t + Vb A} + \Gamma \rho_L \quad (20)$$

where Γ is a correlated liquid distribution coefficient, introduced by Orkiszewski, which implicitly accounts for the following :

- Liquid is distributed in places the slug, the film around the gas bubble and in the gas bubble as entrained droplets.
- The friction loss has two contributions, one from the liquid slug and the other from the liquid film.
- The bubble rise velocity Vb approaches zero as mist flow is approached

The bubble rise velocity Vb was correlated by Griffith and Wallis⁹ as a function of the bubble Reynolds number

$$Nb = 1488 D Vb \rho_L / \mu_L \quad (21)$$

and the liquid Reynolds number

$$N_{RE} = 1488 D Vt \rho_L / \mu_L \quad (22)$$

where Vt is the total superficial velocity given by

$$Vt = V_{SL} + V_{sg} \quad (23)$$

the bubble rise velocity is then calculated from the following set of equations

when $Nb \leq 3000$

$$V_b = (0.546 + 8.74 \times 10^{-6} N_{RE}) \sqrt{g D} \quad (24)$$

when $N_b \geq 8000$

$$V_b = (0.35 + 8.74 \times 10^{-6} N_{RE}) \sqrt{g D} \quad (25)$$

when $3000 < N_b < 8000$

$$V_b = \frac{1}{2} V_{bi} + V_{bi}^2 + \frac{13.59 \mu_L}{\rho_L \sqrt{D}} \quad (26)$$

$$\text{where } V_{bi} = (0.251 + 8.74 \times 10^{-6} N_{RE}) \sqrt{g D} \quad (27)$$

In the Orkiszewski method the friction loss gradient τ_f in the slug regime is calculated from

$$\tau_f = f \frac{v_t^2 \rho_L}{2 g D} \left[\frac{q_L + V_b A}{q_t + V_b A} + \Gamma \right] \quad (28)$$

where the friction factor f is obtained from a Moody diagram as a function of the liquid Reynolds number given by Eq.(22)

The liquid distribution factor Γ is determined using the following equations

when $Vt \leq 10$

$$\Gamma = [(0.013 \log \mu_L) / D^{1.38}] - 0.681 + 0.232 \log Vt - 0.428 \log D \quad (29)$$

when $Vt > 10$

$$\Gamma = [(0.045 \log \mu_L) / D^{0.799}] - 0.709 - 0.162 \log Vt - 0.888 \log D \quad (30)$$

and restricted by the limits

$$\Gamma \geq -0.065 Vt \quad \text{when } Vt \leq 10 \quad (31)$$

$$\Gamma \geq - \frac{Vb A}{q_t + Vb A} \left(1 - \frac{\rho_m}{\rho_L} \right) \quad \text{when } Vt > 10 \quad (32)$$

These restrictions are to avoid pressure discontinuities between flow regimes.

Transition flow

In the transition regime the mixture density ρ_m and the friction loss gradient t_f are calculated for the slug and mist regimes and then weighted with respect to N_g , and L_m and L_s the lower and upper limits of the transition regime, as proposed by Duns and Ros³ :

$$\rho_m = A (\rho_m)_{SLUG} + B (\rho_m)_{MIST} \quad (33)$$

$$t_f = A (t_f)_{SLUG} + B (t_f)_{MIST} \quad (34)$$

where

$$A = \frac{L_m - N_g}{L_m - L_s} \quad (35)$$

and

$$B = \frac{N_g - L_s}{L_m - L_s} \quad (36)$$

Mist flow

In this regime Orkiszewski calculated ρ_m and t_f as Duns and Ross³ :

The density of the mixture is given by

$$\rho_m = (1 - \alpha) \rho_L + \alpha \rho_g \quad (3)$$

where α is obtained assuming negligible slip between phases, then

$$\alpha = \frac{1}{1 + \frac{q_L}{q_g}} \quad (37)$$

The friction-loss gradient is calculated from

$$t_f = f \rho_g V_{sg}^2 / 2 g D \quad (38)$$

where V_{sg} is the superficial gas velocity

In the mist flow regime the friction factor f is obtained from a Moody diagram as a function of the gas Reynolds number

$$N_{RG} = 1488 D V_{sg} \rho_g / \mu_g \quad (39)$$

and a correlated form of the Moody relative roughness factor e/D that was developed by Duns and Ross³. e/D is limited to be bigger than 10^{-3} and less than 0.5.

$$N_w = 4.52 \times 10^{-7} (V_{sg} \mu_L / \gamma)^2 \rho_g / \rho_L \quad (40)$$

if $Nw < 0.005$

$$e/D = 34 \sqrt{\rho_g vsg^2 D} \quad (41)$$

if $Nw > 0.005$

$$e/D = 174.8 \sqrt{Nw}^{0.302} / (\rho_g vsg^2 D) \quad (42)$$

3.4 Single Phase Liquid Flow

In single phase liquid flow the kinetic term will be negligible and for units given in nomenclature,

q.(9) becomes :

$$-dp = \frac{1}{144} \left[\rho_L + t_f \right] dz \quad (43)$$

The calculation of ρ_L has to be done carefully because it represents the most important part of the total pressure gradient. The following procedure has been proposed by Gould⁶

$$\rho_L = 62.4 \gamma_w / Bw \quad (44)$$

where Bw is the formation volume factor of water and is given by :

$$Bw = 1.0 + 1.2 \times 10^{-4} T_x + 1.0 \times 10^{-6} T_x^2 - 3.33 \times 10^{-6} \bar{P} \quad (45)$$

and $T_x = \bar{T} - 60.$

γ_w = specific gravity of water

\bar{T} = Average temperature (°F)

\bar{P} = Average pressure (psia)

The friction loss gradient t_f is obtained from the equation :

$$t_f = \frac{1}{144} f \frac{\rho_L v_L^2}{2 g_c D} \quad (46)$$

where the friction factor f can be calculated by Colebrook¹⁹ equation

$$f = \left\{ 1.14 - 2 \log \left(\frac{e}{D} + \frac{9.28}{N_{RE} \sqrt{f}} \right) \right\}^{-2} \quad (47)$$

where

$$N_{RE} = 1488 D V \rho_L / \mu_L \quad (48)$$

the friction factor f has to be calculated by iteration when using Eq.(47).

3.5 Heat Transfer Equations

When geothermal fluids flow toward the surface there may exist a temperature difference between the formation and the wellbore. This will result in unsteady radial heat transfer.

Ramey²⁰ gives an approximate solution to this problem which permits estimation of fluid and casing temperature as

a function of time. Assuming steady flow in pipe, flow-work is zero, and the total-energy equation can be written as

$$h_i = h_{i-1} - Q + \frac{g}{g_c} \frac{\Delta z}{J} + \frac{\Delta V t^2}{2 g_c J} \quad (49)$$

The amount of heat lost by the fluid and transferred to the ground in an increment of pipe is given by

$$Q = \pi D U (\bar{T} - T_r) \Delta z / W t / f(t) \quad (50)$$

where U (Btu/hr/sqft/F) is the overall heat transfer coefficient and $f(t)$ is a time dependency function expressed by

$$f(t) = -\ln \left(r_c / 2 \sqrt{\alpha' t} \right) - 0.29 \quad (50a)$$

and r_c = is the outer casing radius (ft)

α' = Thermal diffusivity of earth (sqft/day)

t = flowing time (days)

For wells with high flow rates where the convection heat transfer is predominant, the time function cancels out in Eq.(50).

4. COMPUTER CODE

4.1 Description

A computer code has been developed to solve Eq.(9) which determines the pressure drop in a vertical two-phase flow. The code is based on earlier work done by Fandriana et al². When the current effort was initiated it was found that the Fandriana et al² code did not work except for limited input conditions. Also, the calculations were time consuming and therefore costly. The modified computer code takes about ten times less time for execution and accepts a wide range of input conditions. Although the new code is more workable than the previous code, it is limited to use Orkiszewski's method. In the Fandriana et al² code there were options to use the methods of Orkiszewski,¹ Duns and Ros,³ Beggs and Brill, and Hagedorn-Brown.⁴

Pressure drop in two-phase wellbore flow is determined by Eq.(9) which includes the effects of potential energy, friction and acceleration :

$$\Delta P = \frac{1}{144} \left[\frac{\rho_m + t_f}{1 - \frac{Wt q_g}{4637 A^2 p}} \right] \Delta z \quad (9)$$

In the computer code this equation is solved by dividing the total length of the well into intervals where the fluid properties can be considered constant.

The computer code solves a one-dimensional steady-state wellbore model. It includes calculations of the pressure and temperature along with other flowing parameters at different depths. The flowing conditions at the top or bottom of a geothermal well are needed as input. The input data required for the wellbore calculations are shown in Appendix A.2. The computer code solves the pressure drop and the heat transfer Eqs.(9),(49), and (50) simultaneously using simple iteration. The total pressure drop is split into its friction, potential and kinetic terms to show their individual effects. In the code is possible to handle up to eight different diameters with their respective absolute roughness.

A flow diagram of the computer code is given in Appendix A.1. A brief description of the main steps of the code will now be given :

1. Divide the total well length in several intervals.

2. Calculate the rock temperature at the middle of the interval using Lagrange interpolation on the shut-in temperature.
3. Assume a temperature drop, and using Eqs.(49) and (50) calculate enthalpy of mixture.
4. Assume a pressure drop for the interval.
5. Calculate fluid properties for the average pressure and temperature.
6. Calculate the pressure drop using single phase liquid or two-phase flow correlations as needed.
7. Compare with assumed pressure drop, if a good agreement is not achieved repeat from step 4 .
8. Using the calculated pressure drop and assumed temperature drop determine enthalpy of mixture for single phase, and for two-phase use the calculated pressure drop to get the temperature drop.
9. Compare results in step 8 with ones in step 3 if there is not a good agreement repeat from step 3 .
10. Once the pressure and temperature match has

been obtained procede with the next interval.

The calculations end when the total well length has been reached.

The enthalpy of steam and water are obtained from steam tables values using Lagrange interpolation. Steam Density is also calculated from steam tables. The density of the brine is calculated according to Eq.(44). The way in which the remaining variables are obtained can easily be deduced from the program listing in Appendix A. It has to be mentioned that in determining the fluid properties the presence of non-condensable gases is not taken into account. When the geothermal fluid has a high content of non-condensable gases the model should be used with discretion.

While testing the original code developed by Fandriana et al² a jump in the pressure gradient was detected when going from $Vt < 10$ to $Vt > 10$ within the slug regime using the orkiszewski correlation. The jump was partially due to the low viscosities in geothermal wells < 1 cp compared to the high viscosities encountered in oil and gas wells (> 10 cp) for which the correlation was developed. It was found that the cause of this jump was the factor introduced by Orkiszewski to correlate experimental data for the density of two-phase mixtures. In order to give a smooth pressure gradient the next modification in calculating the factor was done:

$$\Gamma = -0.065 Vt - 0.1 \quad (51)$$

and

$$\Gamma = [(0.045 \log \mu_L) / D^{0.799}] - 0.709 - 0.162 \log Vt - 0.888 \log D \quad (30)$$

This second equation restricted by

$$\Gamma \geq - \frac{Vb A}{q + Vb A} \left(1 - \frac{\rho_m}{\rho_L} \right) \quad (32)$$

Eqs. (51) and (30) are evaluated and the bigger value of the factor is to be taken.

This simple procedure became to give a smooth change in pressure gradient and still the agreement with field data was satisfactory.

4.2 Validation

The present computer code was tested against measured pressure and temperature profiles from wells in the Imperial Valley, Cerro Prieto, and Roosevelt Hot Springs.

(a) East Mesa 6-1

The data for this well were obtained from Fandriana et al.² The production zone was set at 7000 ft and the inside pipe diameter 0.7267 ft. The total mass flow rate was

102,500 lb/hr. A pipe roughness of 0.0003 ft was considered in the calculations. The heat transfer coefficient was arbitrarily determined to be 10 Btu/hr/sqft/F and water gravity was taken 1.0208. Appendix B.1 shows the shut-in temperature and measured pressure and temperature profiles of the east Mesa well.

Using the above data, calculations were made starting at bottomhole. The calculated flashing point was at 4079 ft depth showing good agreement with measurements. The calculations showed single phase at the bottom up to flashing point and then going through bubble, slug and transition flow regimes. The superficial velocities at wellhead were 0.987 ft/sec and 107 ft/sec for water and steam respectively. The good agreement with field data can be observed in Fig.1 .

(b) Cerro Prieto M-90

Flowing data for well M-90 in Cerro Prieto was obtained from Castaneda (1983).

The measurements are from a test carried out on February 21st 1978. The production zone was estimated to be at 4261 ft depth. The well has a uniform inside pipe diameter and equal to .5808 ft. The total mass flow rate was 356,840 lb/hr. The pipe roughness was taken as 0.0003 ft. The enthalpy at wellhead was determined to be 578 Btu/lb. The heat transfer to the ground was considered negligible and

the water gravity was assumed 1.019. Table B.2 shows the shut-in temperature as well as the pressure and temperature profiles measured during the the test.

The measured and calculated pressure profile for this well are compared in Fig. 2. The calculations were started at the wellhead using the measured enthalpy, and saturation temperature corresponding to 590 psia. The results showe that well is flowing in two-phase flow. Flashing point was detected at wellbottom. The bubble and slug regimes were observed for these data. It has to be mentioned that using the measured temperature at the wellbottom single phase liquid flow is detected at the bottom but flashing point is calculated at a higher point and the agreement with measured profile is not satisfactory. This may be possible to the high content of CO₂ observed in this well.

(c) Roosevelt Hot Springs 14-2

The data for well 14-2 in Roosevelt Hot Springs were taken from Butz and Plooster¹³, and is a flowing pressure survey identified as log 78-6. For the purpose of our calculations the production interval was considered at 2996 ft. The well has a 0.7433 ft inside diameter casing from surface to bottom. The total mass flow rate at the time of the test was 325,000 lb/hr. The pipe roughness was considered to be 0.0003 ft. An enthalpy of 502 Btu/lb was taken as the average reported in Fig.12 of Butz and

Plooster¹³. The heat transfer to the ground was considered zero. Table B.3 gives the pressure profile for this well; the temperature profile was not available.

The comparison of measured and calculated profiles is shown in Fig.3. The calculations were started at wellbottom. A downhole temperature of 512 F was assumed to match the 502 Btu/lb enthalpy. It can be observed that the agreement is quite good. The flashing point was calculated at 2604 ft, and the bubble and slug flow regimes were observed above the flashing point.

5. USES OF WELLBORE MODELS

5.1 Flowing Pressure and Temperature Profiles

Knowing the discharge conditions and casing schedule of a geothermal well it is possible to calculate the temperature and pressure profiles. Based on these profiles the depth at which the flashing point is occurring can be determined. This point is characterized by a significant change in the pressure gradient.

A good example of the use of temperature profiles is in correlating the kind of minerals that will deposit on the pipe wall at different depths according with the temperatures present at those depths.

In the analysis of mechanical stress on casing and on casing cementing due to thermal effects the temperature profile is required.

The pressure and temperature profile can be useful in determining the depth for setting a pump into the wellbore when needed. Elliot¹² gives a complete analysis of self flowing and pumping geothermal wells, concluding that pumping is not recommendable on an energy basis but it may

be useful in preventing scaling in the wellbore.

The precision of these calculated profiles greatly depends on the quality of input data, Goyal et al²¹ have done some sensitivity studies using Cerro Prieto flowing well data and found that the parameters to be measured, in order of decreasing accuracy, are well inside diameter, wellhead pressure, dryness fraction and mass flow rate. They observed a 70% increase in bottomhole pressure for a 20% decrease in enthalpy.

5.2 Discharge Analysis

The productivity index (PI) is the ratio of the rate of production (Wt) to the pressure drawdown in the reservoir, and is expressed as²³

$$PI = Wt / (p_r - p_{wf}) \quad \text{lb/hr/psi} \quad (52)$$

It is a measure of the ability of the well to flow. p_r is the static reservoir pressure and can be obtained using well test analysis techniques or by a sufficiently long shut-in time. p_{wf} is the wellbottom flowing pressure and can be measured using subsurface pressure instruments, or using a wellbore flow model and wellhead measurements.

In calculating the discharge curve of a geothermal well and the effect of the productivity index on it we consider

that flow in the reservoir is steady state or semi-steady state, We can then consider the PI constant for a wide range of pressure drawdown as long as the fluid in the reservoir is flowing as single phase liquid.

As an example of how the wellbore model can be applied in calculating discharge curves data from Svartsengi well # 12 in Iceland²⁴ will be used. Table I shows the data for this well .

TABLE I . Data for Svartsengi well # 12 in 1983

Pwh = 220.6 psia

Twh = 390.3 °F

Wt = 333,432 lb/hr

h_m = 429.12 Btu/lb

Wellbottom = 3936 ft

Øi of pipe = 1.0521 ft from 0 to 1991 ft

Øi of bare-hole = 1.0208 ft from 1991 to bottom

Reservoir pressure = 1279 psia

With these data and considering heat transfer negligible the wellbore model predicted a flowing wellbore pressure of 1050 psia. Using Eq.(52) a PI of 1456 lb/hr/psi was calculated. Knowing the PI and considering it constant, several wellbottom flowing pressures were calculated for different total mass flow rates. Using the wellbore model these

wellbore flowing pressure were corrected for wellhead conditions.

Fig. 4 shows the characteristic production curve for the original 1456 lb/hr/psi PI. It also shows the curves for 500 and 1000 lb/hr/psi assumed PI's. As can be observed the decline of the discharge curve with respect of wellhead pressure is bigger for low than for high productivity indexes. Analyzing additional data from the computer output it was observed that for low productivity indexes the pressure drop in the wellbore represents a small fraction of the total available pressure. The same observation has been made by Butz et al¹³.

5.3 Casing Design

Wellbore flow models can be very useful in the design of casing schedules. To observe the effect of inside diameter in the wellbore performance several runs were made for Svartsengi well # 12 using the data given in Table I assuming that the well is totally cased with a same casing to bottom and using an arbitrarily PI of 1280 lb/hr/psi. Three different diameters were assumed 13 3/8", 9 5/8", and 7 5/8" which are commonly used in geothermal wells.

From Figs. 5, 6, and 7 it can be seen that for a given flowrate the wellhead pressure is lower for a smaller

diameter due to an increase in friction losses. In these figures, A is pressure drop in reservoir, B is pressure drop due to potential in single phase liquid, C is the pressure drop due to friction in single phase liquid, D is pressure drop due to potential in two-phase flow, and D is the pressure drop due to friction in two-phase flow.

Svartsengi well # 12 presents an interesting case in which for low flow rates the pressure at wellhead increases with increasing flowrate, this occurs up to a maximum discharge pressure at which for higher flow rates pressure wellhead decreases as expected. This behavior has been noticed in measured output curve for other similar wells in the Svartsengi field.²⁴

From Figs. 5, 6, and 7 We observe that increasing wellhead pressure with increasing flow rate tends to disappear for small diameter. It can also be noticed that the pressure drop due to potential effects in two phase-flow is diminishing for small diameters for which We have higher velocities . This may be due to the fact, that in contrast to single phase liquid flow an increase in diameter or decrease in flow rate in two-phase flow does not necessarily represents a reduction in pressure gradients. This is because of the presence of gas (steam) which slips through the liquid without contributing to the lift.

Finally, We note that below the flashing point the pressure drop is mainly controlled by the potential term so

the casing size is not as critical as in two-phase flow.

5.4 Reservoir Fluid Enthalpy

To analyze the effect of the reservoir fluid enthalpy in the performance of a geothermal well, several runs were made using data for Svartsengi well # 4 given in Table II.²⁴

TABLE II . Data for Svartsengi Well # 4 in 1975

$$P_{wh} = 263.04 \text{ psia}$$

$$T_{wh} = 405.54 \text{ F}$$

$$W_t = 467,280 \text{ lb/hr}$$

$$h = 454.2 \text{ Btu/lb}$$

$$\text{Wellbottom} = 3,359 \text{ ft}$$

$$O_i \text{ of pipe} = 0.7218 \text{ ft from 0 to 1148 ft}$$

$$O_i \text{ of pipe} = 0.5676 \text{ ft from 1148 to bottom}$$

The overall heat transfer coefficient was considered negligible. Using the wellbore model a bottom hole pressure of 1067 psia and a temperature of 472 F were calculated. Considering everything constant the wellbottom temperature was increased to simulate an increase in reservoir fluid enthalpy. The increase in temperature was taken to a point in which the flashing occurs a few feet above the wellbottom. It was not increased more because if flashing

occurs at the reservoir then the productivity index can not be considered constant anymore.

From Fig.8 it can be seen that wellhead pressure depends greatly on the reservoir fluid enthalpy. Bilicki et al¹⁴ have concluded that reservoir temperature is a decisive parameter in the flow performance of geothermal wells.

Wells producing from two-feed zones in a steady-flow can be analyzed using wellbore models. The well performance will depend on the enthalpy of the fluids entering the well. Grant et al,²⁵ refer to the case of two-feed zones, showing in a schematical way how a well with an upper steam-feed and a water lower-feed will cycle when operated at low flow rates. A well with a cold water entrance may stop flowing or diminish its flow performance due to lowering of mixture enthalpy.

5.5 Scale Deposition

Scale deposition such as calcium carbonate will normally occur immediatly above the flashing point. This deposition can occur in a length of several feet and form rapidly causing a decrease in flow rate or in wellhead pressure even when the reservoir characteristics remain practically constant.

The wellbore model was used to simulate scale deposition in Svartsengi well # 4 with the data given in Table II. The scale deposition was assumed to occur in the 300 ft immediately above the flashing point which was calculated at 1890 ft. The incrustated interval was assumed to have a constant diameter and the roughness was considered 0.003 ft which is an average for concrete. The mass flow rate, wellbottom flowing pressure and the productivity index were kept constant so the flashing point remained at the same depth.

Fig.9 shows the reduction in wellhead pressure as a function of the fraction of cross-sectional area that has been incrustated. It can be noticed that this curve is concave downwards in contrast with a production decline curve which would probably be concave upwards. This behavior of incrustation has been observed in Svartsengi. The present wellbore model and approach have been applied²⁶ to wells in the Miravalles geothermal field in Costa Rica. A good match with field data has been achieved. Grant et al,²⁷ mention that an increasing decline in flow as flow approaches zero is characteristic of deposition.

It remains to determine the rate of deposition. Usually is assumed that the volume of scale deposited per unit length will increase linearly with cumulative production²⁴. Then using this criteria the pressure drop at the wellhead would decrease slightly at the beginning of incrustation and

declining faster as more and more area has been incrustated.

5.6 Wellbore Heat Transfer

When obtaining the characteristic production curves of a geothermal well in a short time the enthalpy of the mixture increases with flow rate and shows a reduction at low rates. This has been observed in the Los Azufres geothermal field in Mexico²⁸. If we look at Eq.(50) we notice that for high flow rates and low wellbore temperature the amount of heat transferred to the ground decreases. If the shut-in temperature and the remaining reservoir/fluid parameter are known the overall heat transfer coefficient can perhaps be estimated by matching the measured and calculated profiles.

For geothermal wells with commercial flow rates the formation around the well reaches thermal equilibrium after few days or weeks in most instances, the heat conduction can then be neglected in our calculations.

Fig.10 gives effect of heat transfer on the pressure profile at well 6-1 in East Mesa field. The curve to the left was calculated assuming an overall heat transfer coefficient of 10 Btu/hr/sqft/F but the other curve assuming zero heat transfer. It can be noticed that the curve with overall heat transfer coefficient equal zero will flash at a deeper point and also will have a higher pressure at the

wellhead because of its higher enthalpy.

5.7 Well Test Analysis

Transient pressure test have been used with good results in oil and gas industry and have become an important technique to obtain reservoir data. Unfortunately these analytical and graphical techniques are based on bottomhole pressure measurements which are very difficult to obtain in geothermal wells.

Hoang¹⁶ approaches the problem using a wellbore flow model to calculate wellbottom pressures and couples them with a simple reservoir simulator. He assumes steady-state flow in the wellbore and single fluid phase flowing in a radial form in the reservoir. The permeability and porosity are considered uniform anywhere in the reservoir. A good agreement was obtained in comparing simulated reservoir parameter in this form and the ones obtained by means of the conventional well test techniques.

Miller¹⁵ has coupled a transient wellbore model with a simple reservoir model. A single phase liquid flow was assumed at the reservoir and single or two phase flow in the wellbore. Calculation using this approach have been made obtaining interesting results but no matching with field data were reported.

5.8 Decline Curves

Production decline curves provides a simple method for predicting the future behavior and life of a reservoir. They are based on the assumption that reservoir behavior can be determined from any mathematical relationship that can be matched to the production history. The usual method is to plot the production rate of unrestricted wells against the production time and then extrapolate the resultant curve for estimating future behavior.

When a well has been producing in a restricted way the obtainment of decline curves is not possible. Cutler and Johnson³⁰ proposed for oil wells the use of bottomhole pressures and productivity index data for calculating the production decline curve that the well would have followed if it were allowed to produce without restriction.

Because of the lack of a physical model supporting decline curve methods their uses appear limited²⁵. They can not predict the effects of changes in management practice or the character of the reservoir such as cold water entry. However, many successful predictions have been made using this simple method .

CONCLUSIONS

1. A workable computer code has been developed to simulate vertical two-phase flow in geothermal wells. Reasonable results can be obtained when the input data are of good quality.
2. Using the computer code the output characteristic curve can be obtained considering constant productivity indexes.
3. In casing design is very useful to split the total pressure gradient in its potential, friction and kinetic terms to observe its individual effects. In single liquid phase flow the casing diameter is not critical because the pressure drop is mainly controlled by the potential term.
4. The reservoir temperature is a very important parameter in well flow performance in the liquid dominated reservoir.
5. The wellbore flow models can be applied to analyze the effect of cold water entrance in wellbores.
6. A good example of use has been in simulating

scale deposition.

7. The use of wellbore flow models in the obtaining reservoir characteristics seems to be limited due to the high resolution needed in well test analysis techniques.
8. Wellbore flow models can be used in obtaining of overall heat transfer coefficient when the pressure and temperature profiles are matched.
9. The model can be used in evaluating production histories to analyze them using production decline curves.

NOMENCLATURE

A	cross-sectional area of pipe, sqft
D	inner pipe diameter, ft
e	absolute roughness of pipe, ft
f	Moody friction factor, dimensionless
g	gravity acceleration, ft/sec
g_c	gravitational constant, ft-lbm / lbf-sec
h	enthalpy, Btu/lbm
J	Mechanical equivalent of heat (778 ft-lbf / Btu)
L_m	lower limit mist flow, dimensionless
L_s	higher limit slug flow, dimensionless
N_b	bubble Reynolds number, dimensionless
N_g	gas number, dimensionless
N_L	liquid number, dimensionless
N_{Re}	Reynolds number, dimensionless
p	pressure, psia
Q	heat transfered to surroundings, Btu /lbm
q	volumetric flow rate, ft / sec
t	time, sec
t_f	friction-loss gradient, lb/ft /ft
U	overall heat transfer coeff., Btu/hr/sqft/F
V	velocity, ft/sec
V_b	bubble rise velocity, ft/sec
V_s	slip velocity, ft/sec
V_{sg}	superficial gas velocity
V_{sl}	superficial liquid velocity, ft/sec
W_t	total mass flow rate, lbm/hr

x steam quality, dimensionless
z depth, ft
 α void fraction, dimensionless
 δ_w specific gravity of water, dimensionless
 Γ liquid distribution coeff., dimensionless
 ρ density, lbm/ft³
 σ surface tension, dynes/cm
 τ_w shear stress, lbf/sqin
 μ viscosity, cp.
 ν specific volume, ft³/lbm

Subscripts:

f and L liquid
fg vaporation
g gas
m mixture
t total

REFERENCES

1. Orkiszewski, J.: " Predicting Two-Phase Pressure Drops in Vertical Pipes," Journal of Petroleum Technology (June 1967).
2. Fandriana, L., Sanyal, S.K., Ramey, H.J.Jr.: " A Numerical Simulator for Heat and Fluid Flow in a Geothermal Well," Petroleum Department Report, Stanford University, Stanford CA. (Oct 1981).
3. Duns, H.Jr., Ros, N.C.J.: " Vertical Flow of Gas and Liquid Mixtures in Wells," Proc. Sixth World Pet. Congress, Frankfurt, (June 19-26 1963), Section II, paper 22-PD 6.
4. Hagedorn, A.R., Brown, K.E.: " Experimental Study of Pressure Gradients Occurring During Continuous Two-Phase Flow in Small Diameter Vertical Conduits," J. Pet. Tech., (April 1965), 475-484.
5. Aziz, K., Govier, G.W., Fogarasi, M.: " Pressure Drop in Wells Producing Oil and Gas," J.Cdn.Pet.Tech., (Sept 1972), 38-48.
6. Gould, T.L.: " Vertical Two-Phase Steam-Water Flow in Geothermal Wells," J.Pet.Tech., (Aug 1974), 833-842.
7. Poettmann, F.H., Carpenter, P.G.: " The Multiphase Flow of Gas, Oil and Water Through Vertical Flow Strings With

- Application to The Design of Gas-Lift Installation,"
Drill.and Prod.Prac.,API, (1952), 257-317.
8. Wallis,G.B.: " One-Dimensional Two-Phase Flow," McGraw Hill (1969).
 9. Griffith,P.,Wallis,G.B.: "Two-Phase Slug Flow," J.Heat Transfer, Trans. ASME, (Aug 1961), 307-320.
 10. Upadhyay,R.N.,Hartz,J.D.,Tomkoria,B.N.,Gulati,M.S.: " Comparison of the Calculated and Observed Pressure Drops in Geothermal Wells Producing Steam-Water Mixtures," SPE of AIME, Paper SPE 6766. 52nd Annual Fall Tech. Conf. and Exhibition, Denver,Co.,(Oct 9-12, 1977).
 11. Nathenson,M.: " Flashing Flow in Hot-Water Geothermal Wells," J. Research U.S.Geological Survey (Nov-Dec 1974) Vol.2, No.6, 743-751.
 12. Elliot,D.G.: " Comparison of Brine Production Methods and Conversion Processes for Geothermal Electrical Power Generation," Enviromental Quality Laboratory Report No.10, California Institute of Technology (July 1975).
 13. Butz,J.,Plooster,M.: " Subsurface Investigations at the Roosevelt KGRA, Utah," Final report DOE/ET/28389-1 (Oct 1979)
 14. Bilicki,Z.,DiPippo,R.,Kestin,J., Maeder,P.F., Michaelides,E.E.: " Available Work Analysis in the Design of Geothermal Wells," International Conference on

Geothermal Energy, Paper H4 (May 11-12, 1982) Florence Italy.

15. Miller, C.W.: " Numerical Model of Transient Two-Phase Flow in a Wellbore," Lawrence Berkeley Laboratory, LBL-9056, (1979) Berkeley, CA.
16. Hoang, V.T.: " Estimating Reservoir Properties and Well Performance Using Surface Production Data," Eighth Annual Workshop Geothermal Reservoir Engineering (Dec 1982) Stanford University, Stanford CA.
17. Reynolds, W.C., Perkins, H.C.: " Enginnering Thermodynamics" McGraw Hill (1977) Second edition.
18. Chierici, G.L., Giannone, G., Sclocchi, G., Terzi, L.: " A Wellbore Model for Two-Phase Flow in Geothermal Reservoirs," Paper SPE 10135 (1981).
19. Vennard, J.K., Street, R.L.: " Elementary Fluid Mechanics," John Wiley and Sons, Fifth edition (1975).
20. Ramey, H.J.: " Wellbore Heat Transmition," J.Pet.Tech. (April 1962) 427-435 ; Trans. AIME 225.
21. Goyal, K.P., Miller, C.P., Lippmann, M.J.: " Effect of Measured Wellhead Parameters and Well Scaling on the Computed Downhole Conditions in Cerro Prieto Wells," Sixth Workshop on Geothermal Reservoir Engineering (Dec 1980) Stanford University, Stanford CA.

22. Barelli, A., Corsi, R., DelPizzo, G., Scali, C.: " A Two-phase Flow Model for Geothermal Wells in Presence of Non-condensable Gases," Geothermics, Vol 11, No.3, (1982) pp. 175-191
23. Craft, B.C., Hawkins, M.F.: " Applied Reservoir Engineering," Prentice-Hall, Inc. (1959).
24. Gudmundsson, J.S.: " Personal communication " (1983)
25. Grant, M.A., Bixley, P.F., Syms, M.C.: " Instability in Well Performance," Geothermal Resources Council, Trans., Vol.3 (Sep 1979). 275-278.
26. Granados, E.: " Personal communication " (1983)
27. Grant, M.A., Donaldson, I.G., Bixley, P.F.: " Geothermal Reservoir Engineering " Academic Press (1982)
28. Coordinadora Los Azufres, Mexico: " Internal Reports "
29. Sanyal, S.K., Brown, S., Fandriana, L.: " Sensitivity Study of Variables Affecting Fluid Flow in Geothermal Wells," Fourth Workshop Geothermal Reservoir Engineering, (Dec 1978) Stanford University, Stanford CA.
30. Cutler, W.W., Johnson, H.R.,: " Estimating Recoverable Oil of Curtailed Wells," Oil Weekly (May 27, 1940)
31. Ryley, D.J., Parker, G.J.: " Flowing Geothermal Wells: Cerro Prieto Well M-91 and Krafla Well KJ-91 ; Computer Analysis Compared with Experimental Data," International

Conference on Geothermal Energy, Florence Italy (May
11-14, 1982) Paper C4, 187-194.

32. Castaneda,M.: " Personal communication " (1983).

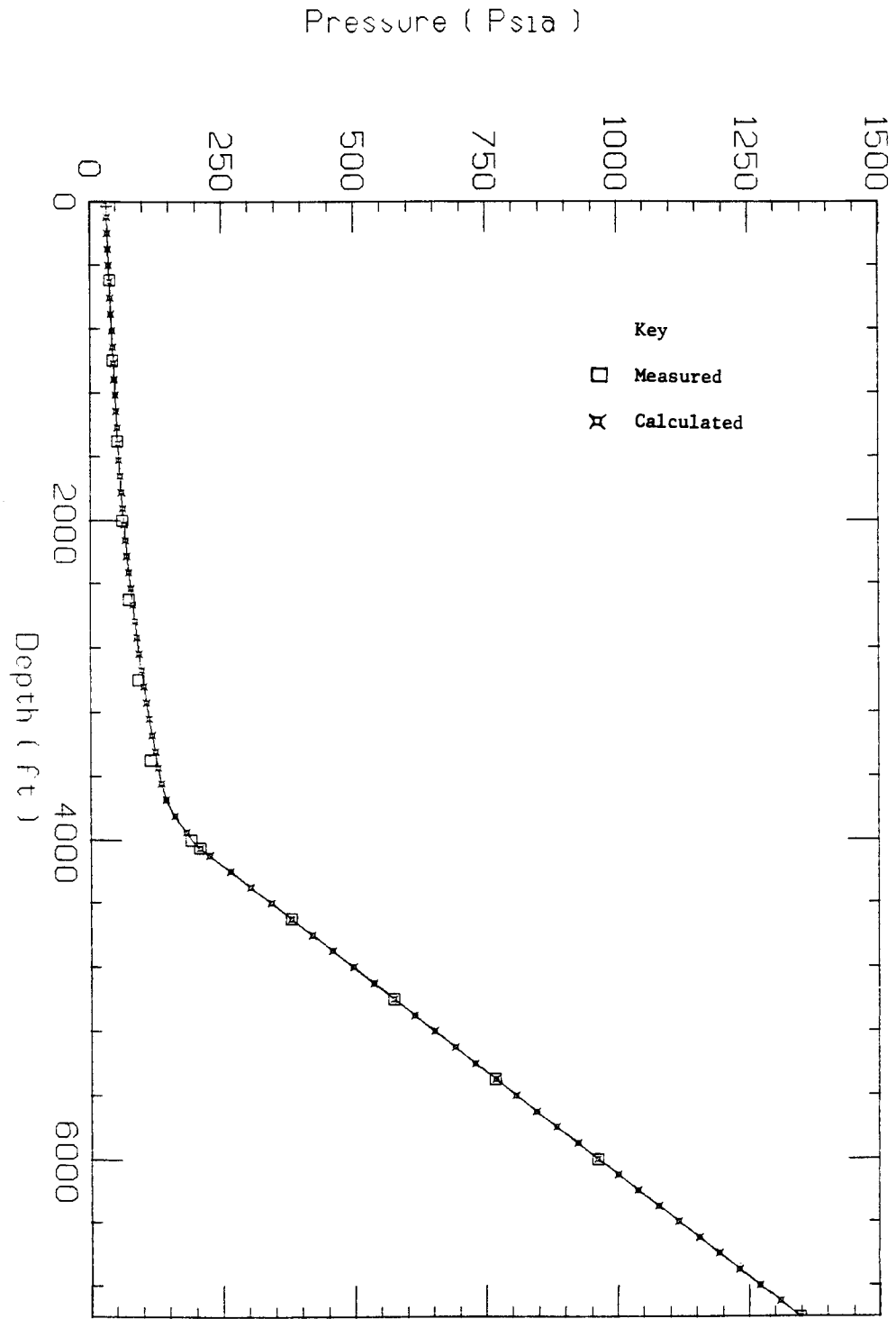


Fig. 1. Measured and Calculated Flowing Pressure Profile for Well East Mesa 6-1.

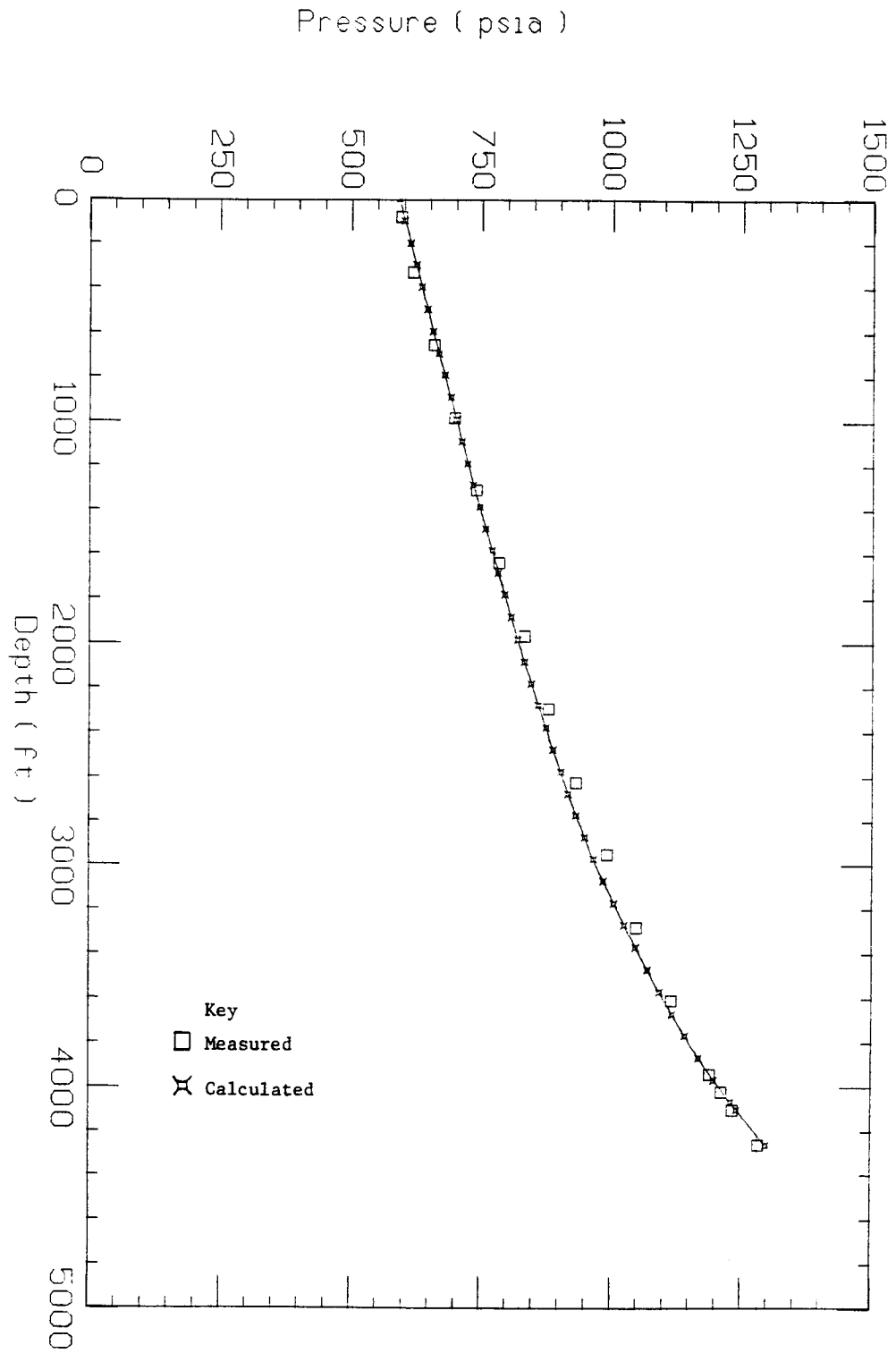


Fig. 2. Measured and Calculated Flowing Pressure Profile for Well M-90.

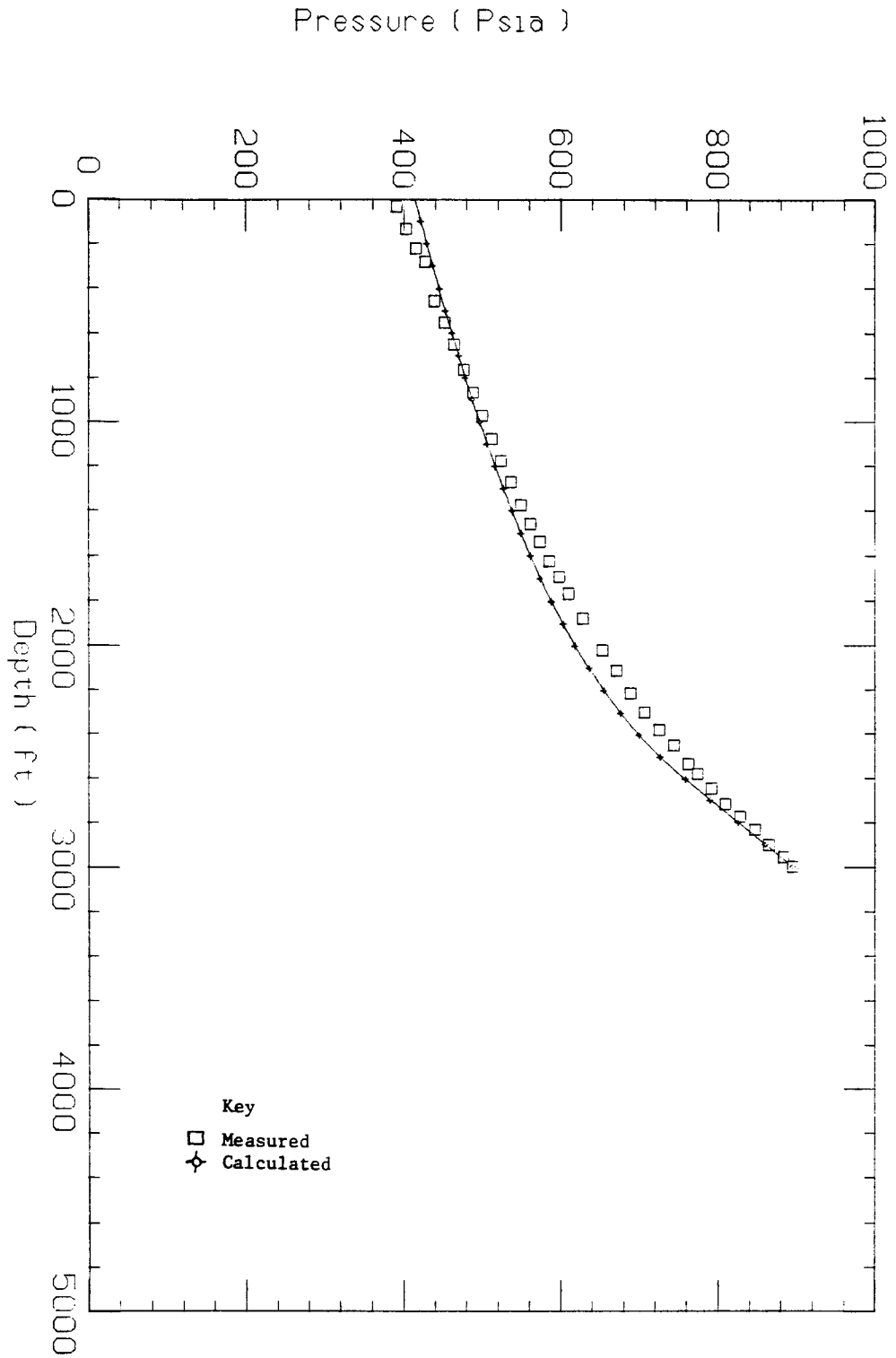


Fig. 3. Measured and Calculated Flowing Pressure Profile for Well Roosevelt Hot Springs 14-2.

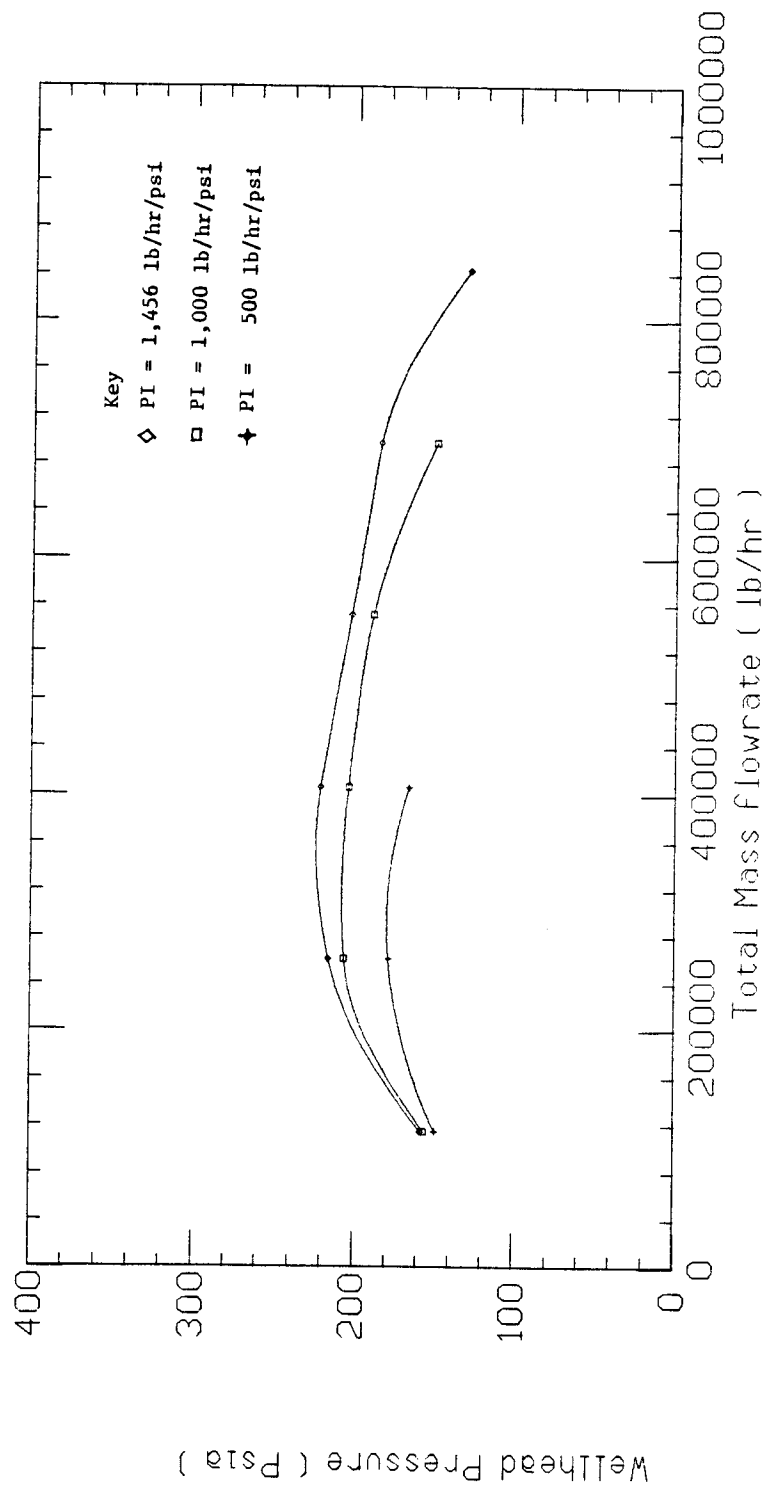


Fig. 4. Characteristic Production Curves for Svartsengi Well 12.

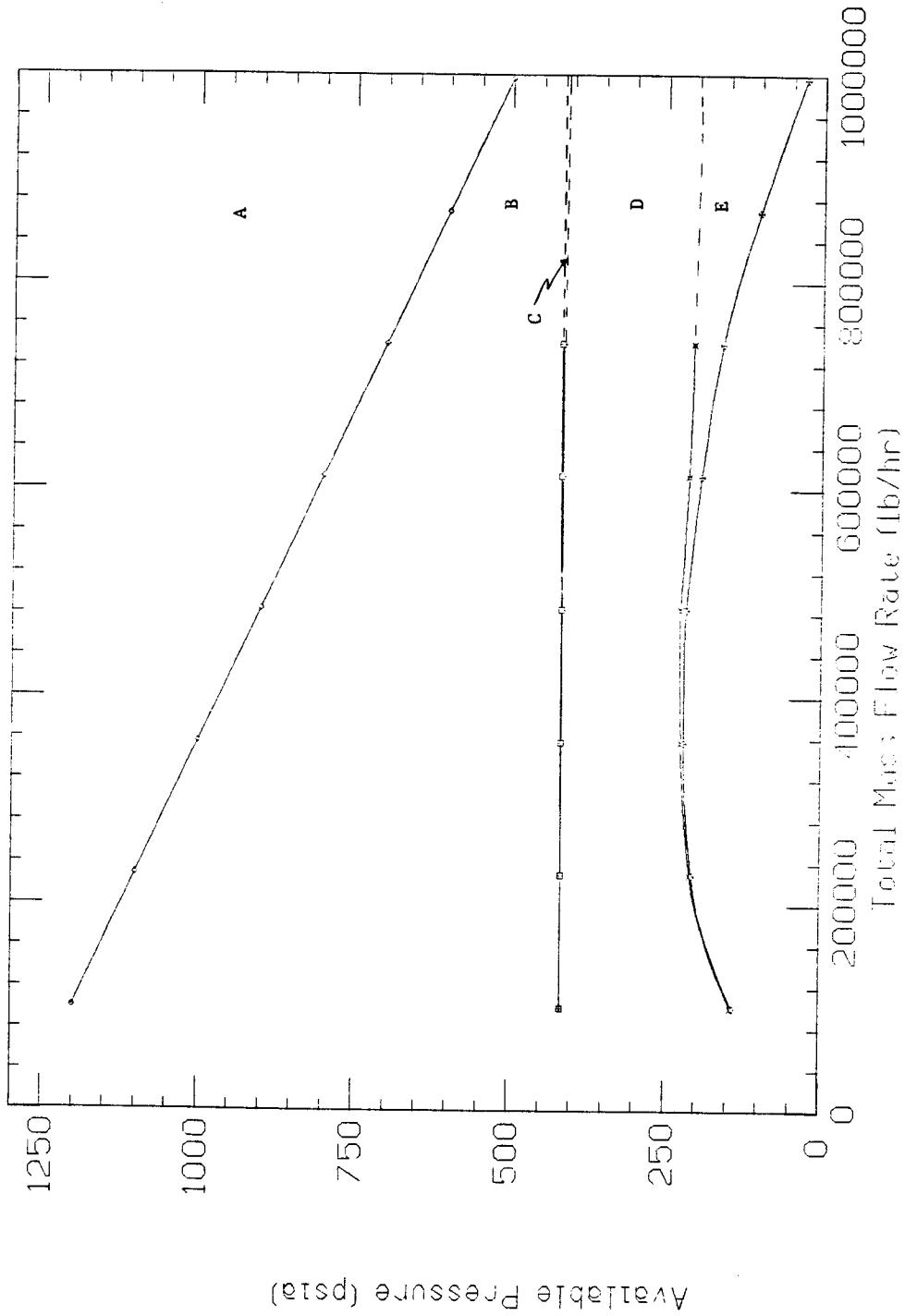


Fig. 5. Available Pressure Curves for Svartsengi Well 12. Assuming a Single 13 3/8" Casing to Bottom.

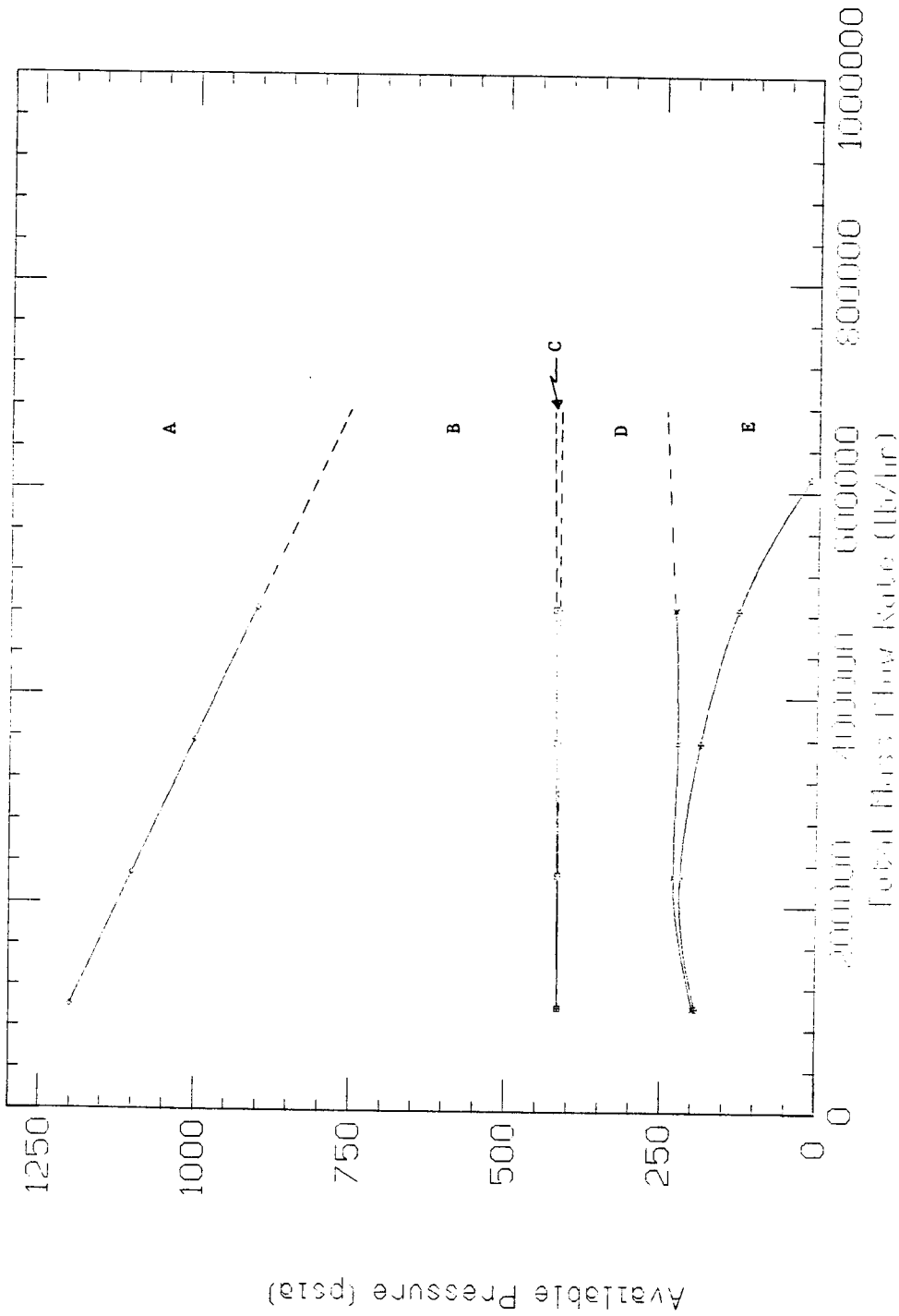


Fig. 6. Available Pressure Curves for Svartsengi Well 12.
Assuming a Single 9 5/8 " Casing to Bottom.

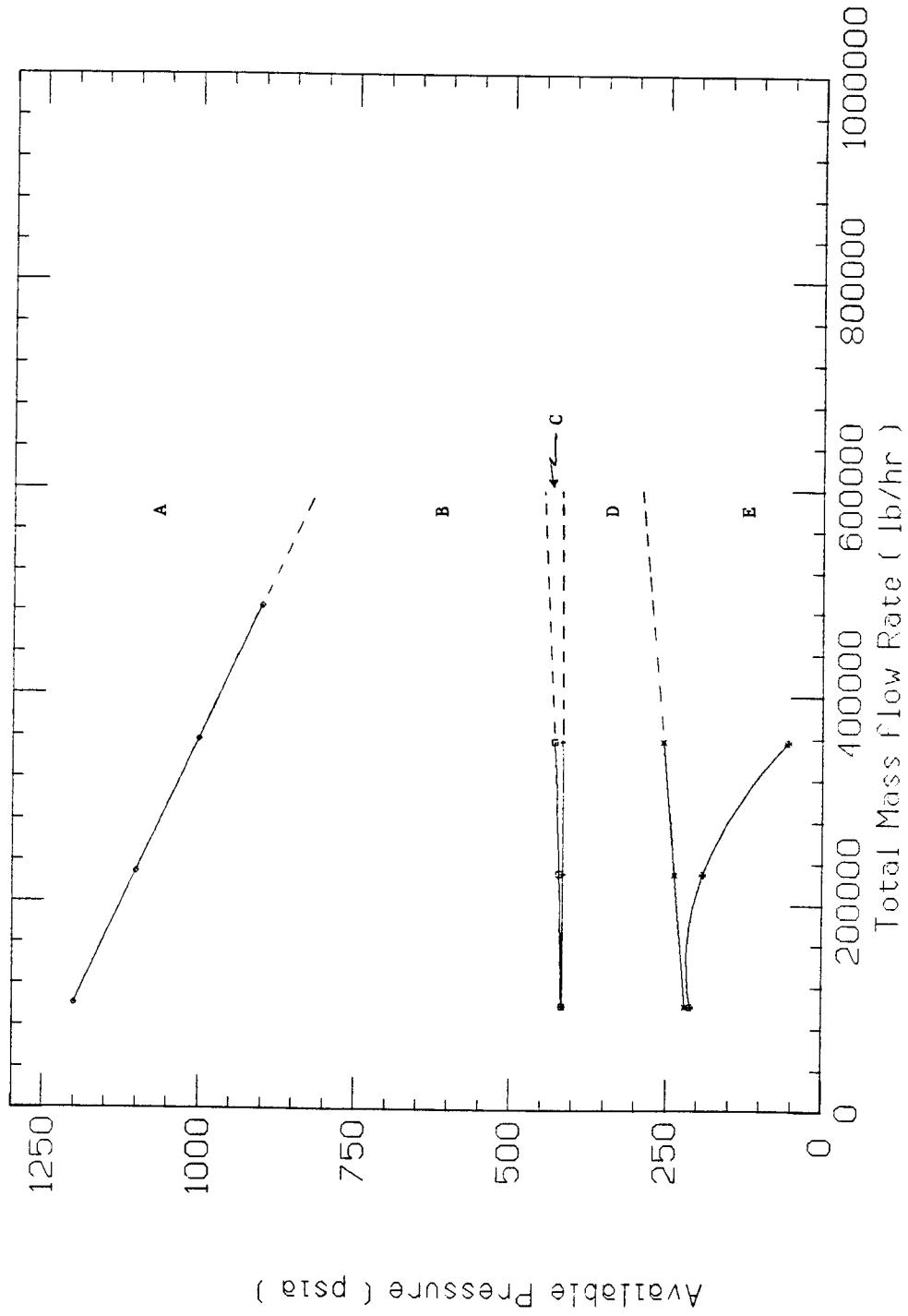


Fig. 7. Available Pressure Curves for Svartsengi Well 12. Assuming a Single 7 5/8" Casing to Bottom.

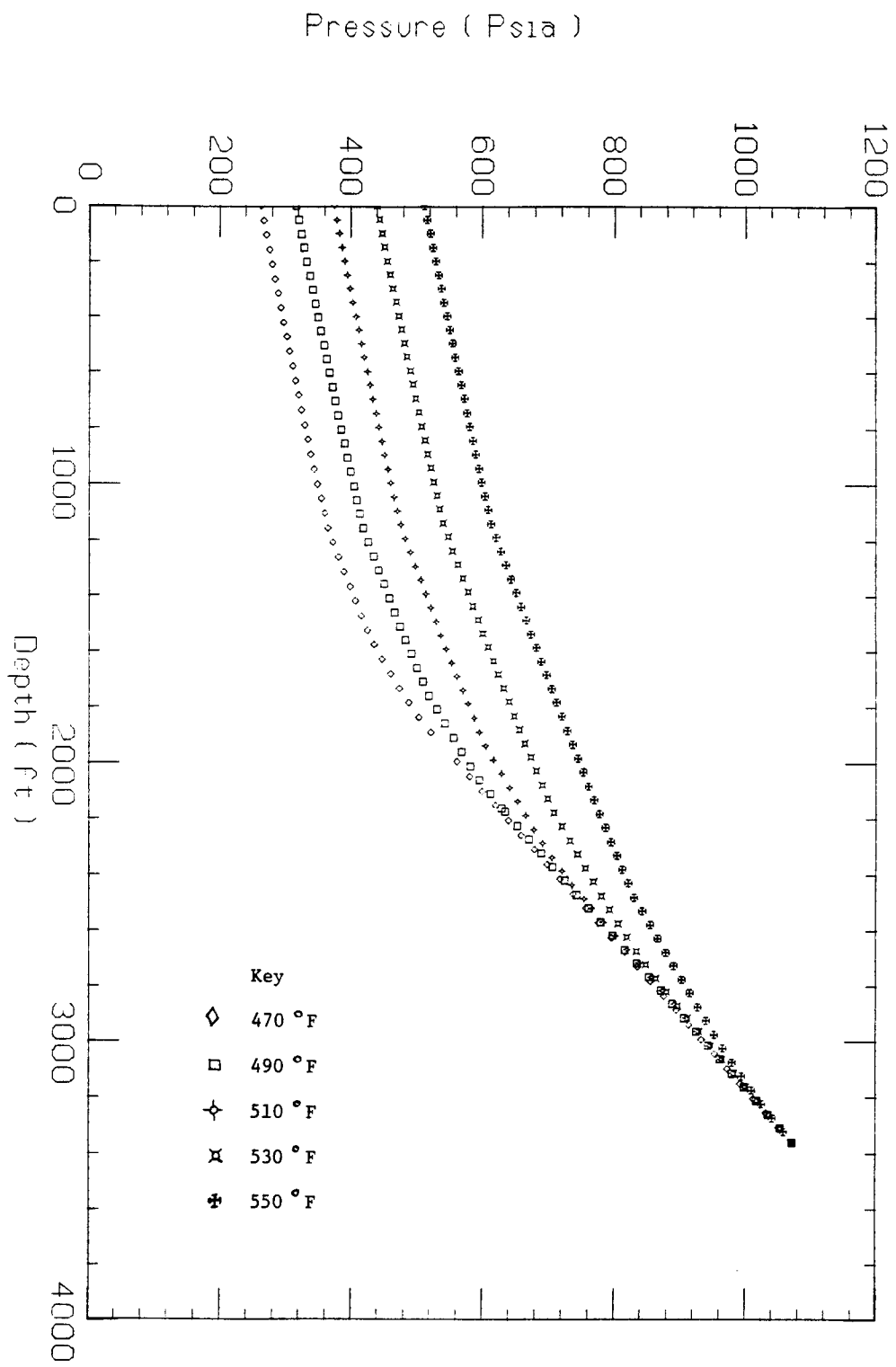


Fig. 8. Calculated Pressure Profiles Showing the Effect of Fluid Enthalpy in Svartsengi Well 4.

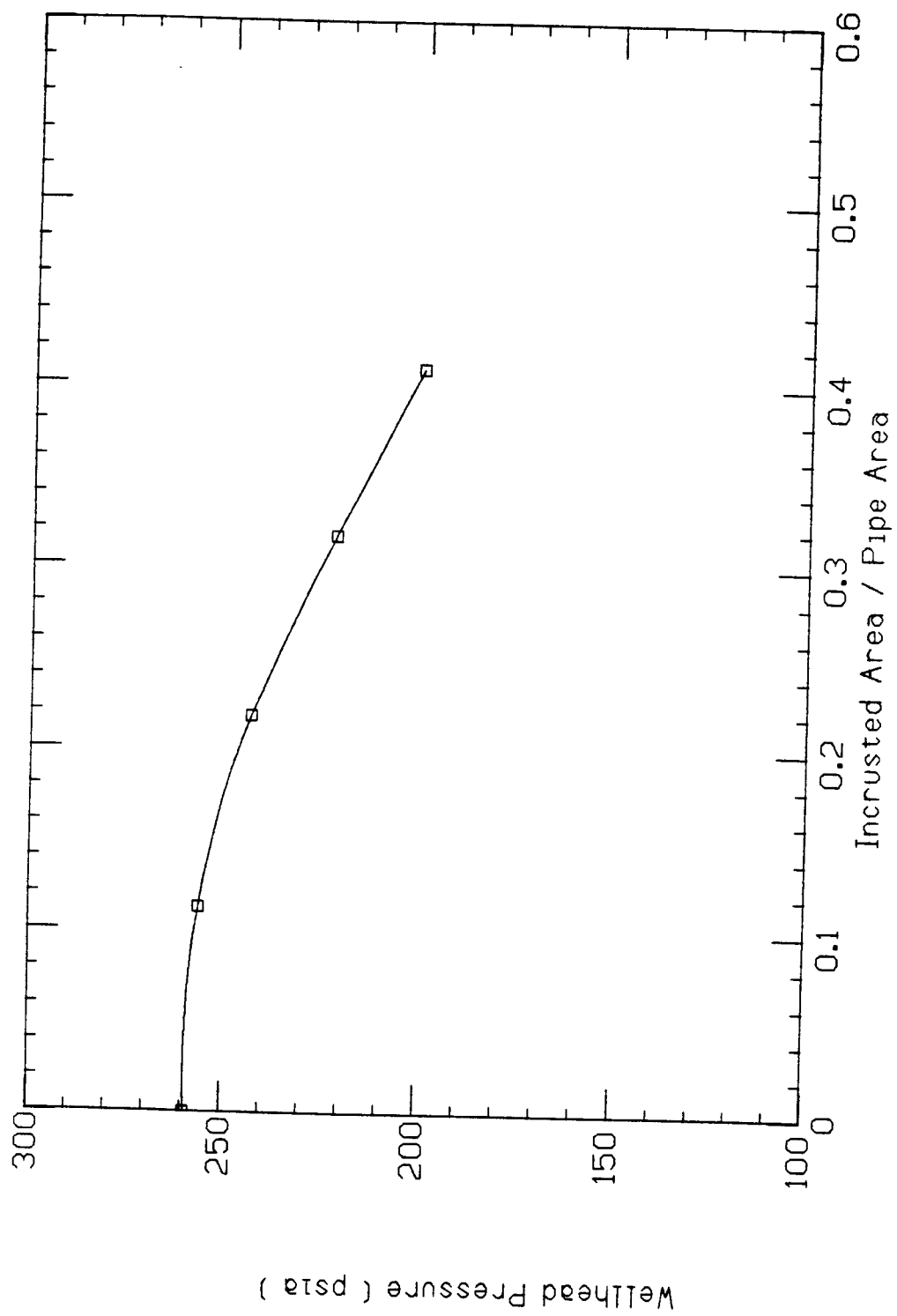


Fig. 9. Scale Deposition Simulation for Svartsengi Well 4.

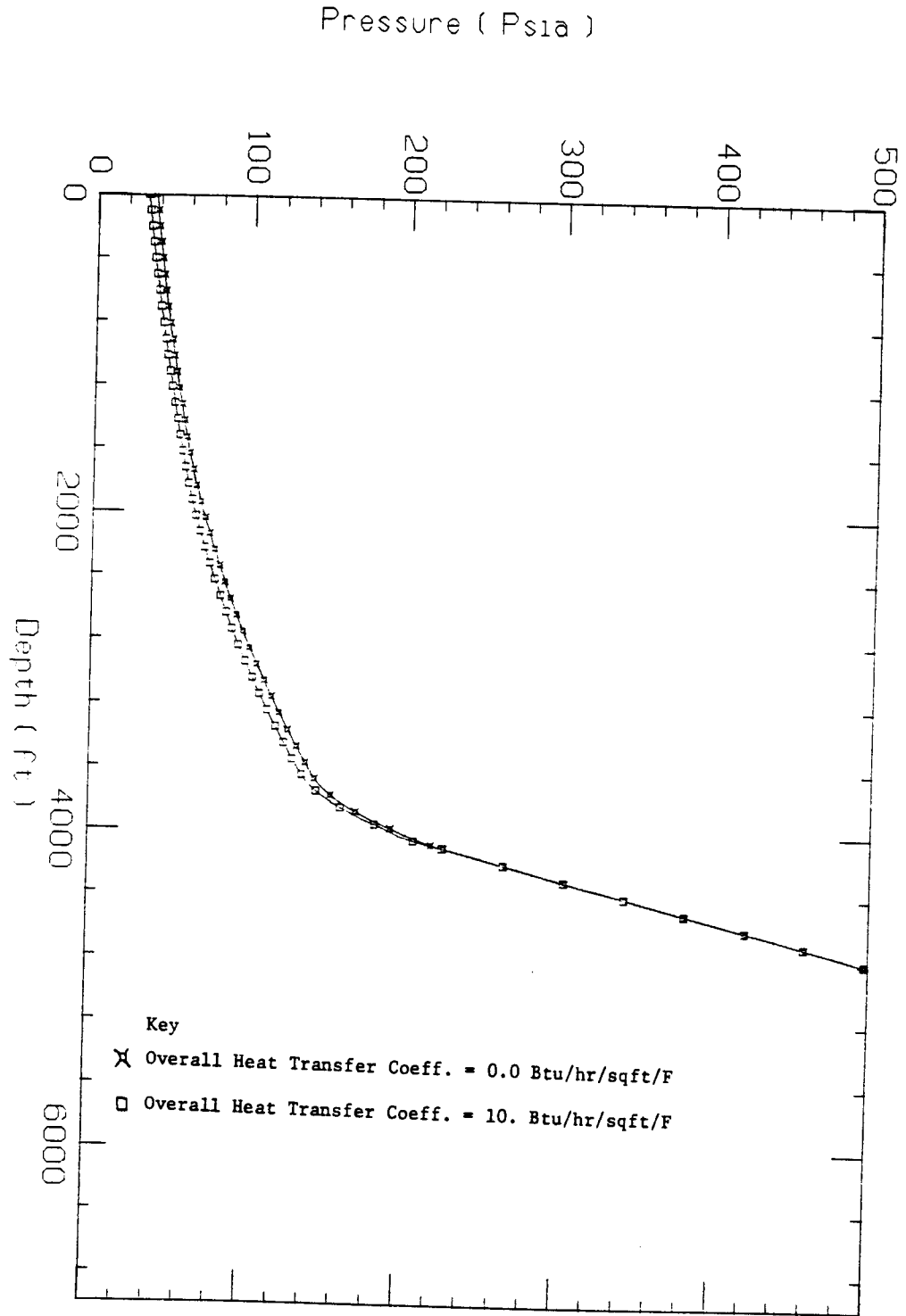
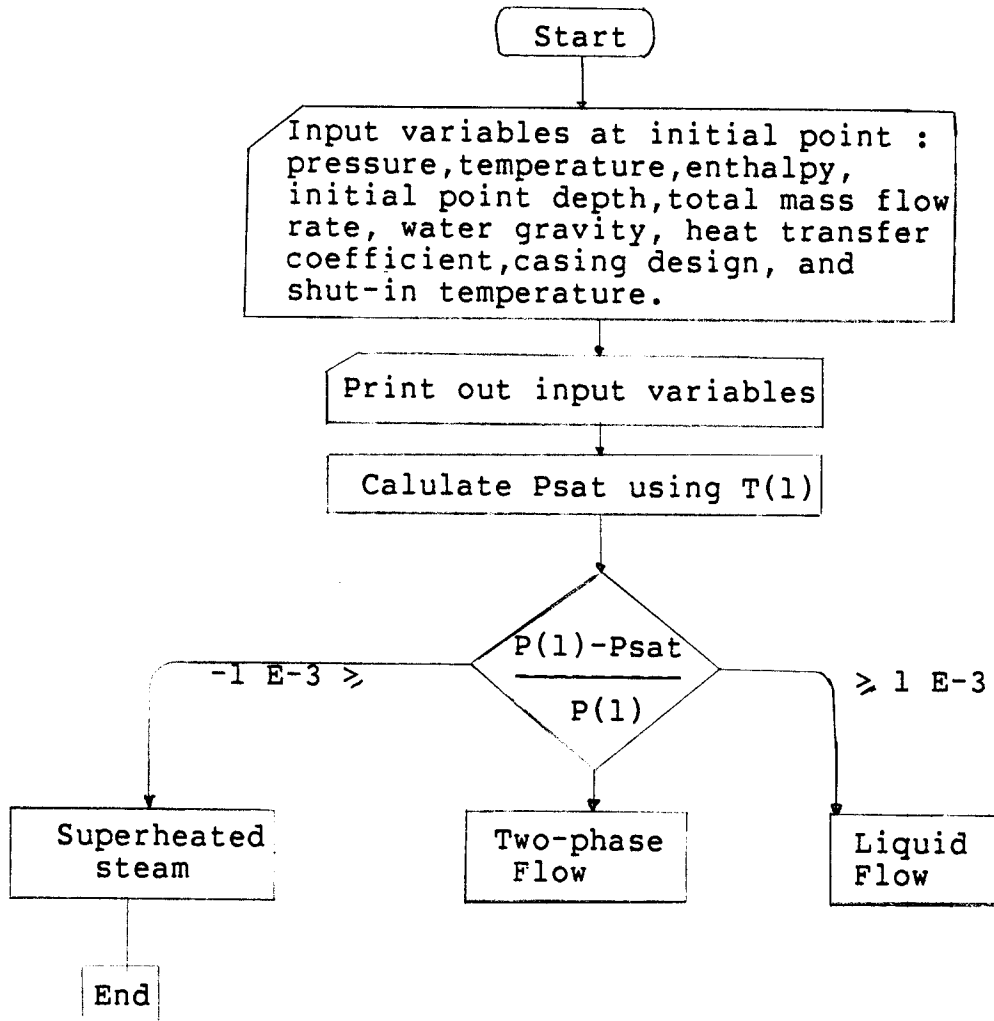
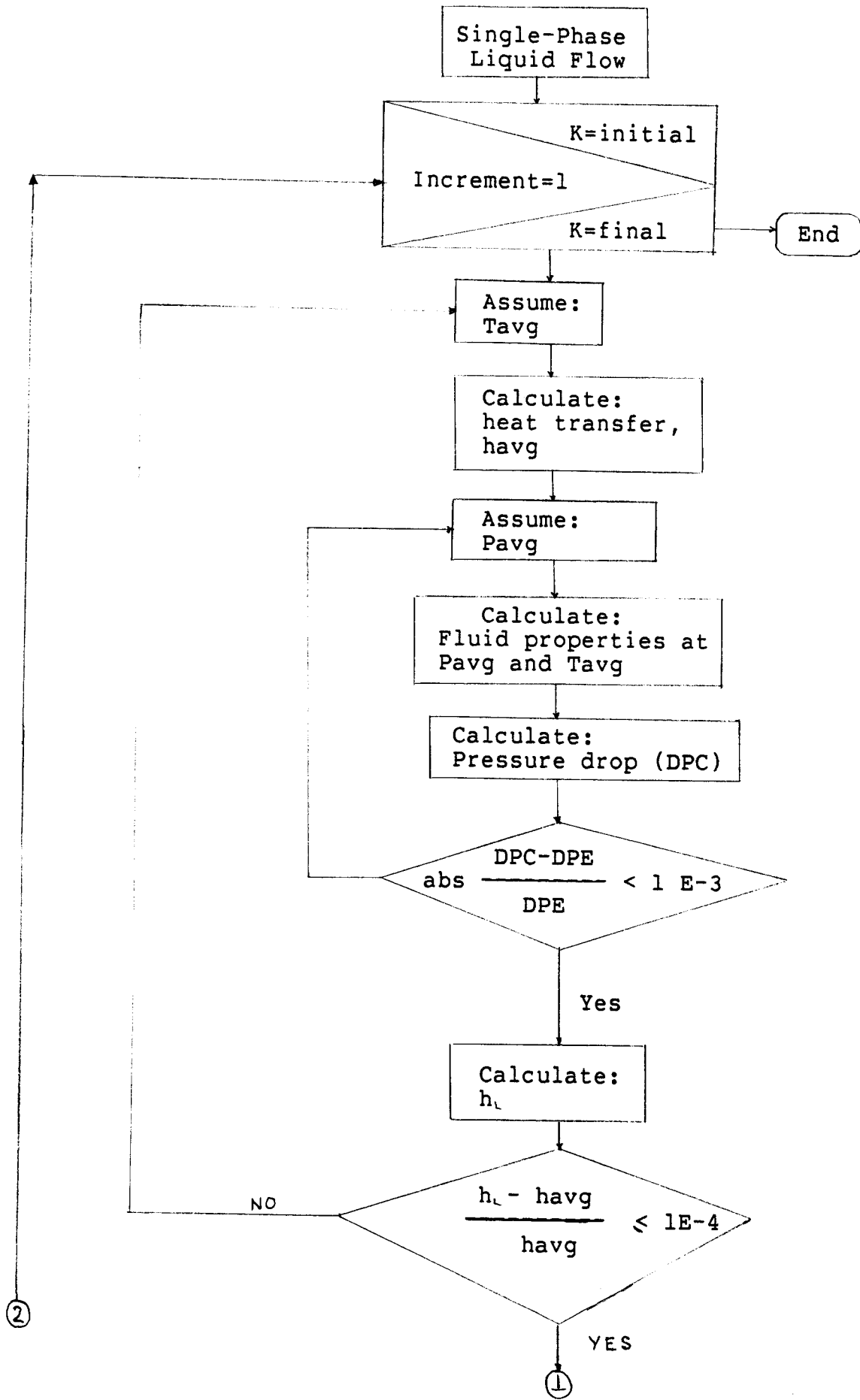


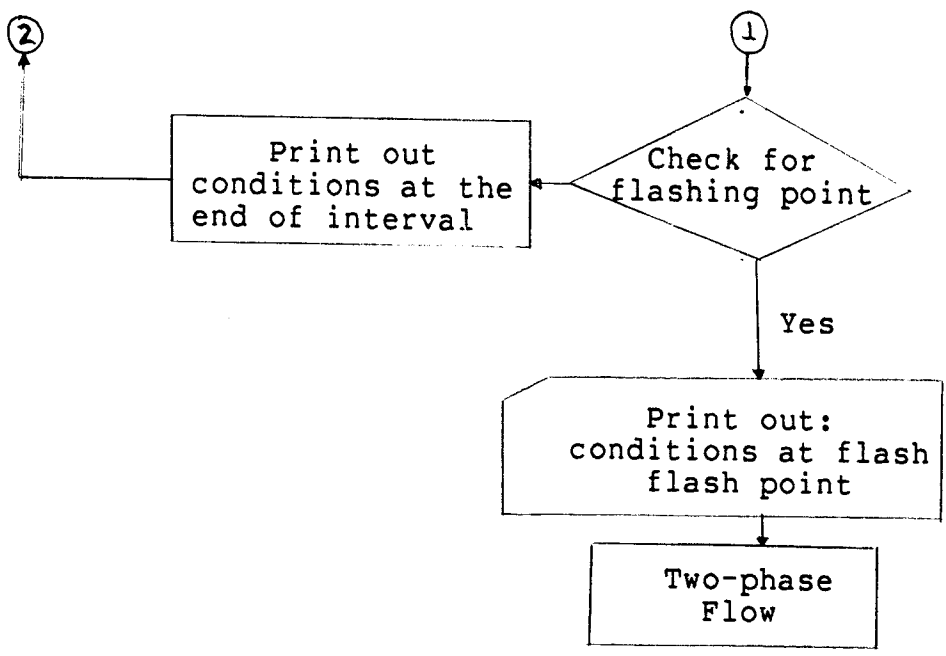
Fig. 10. Calculated Pressure Profiles to observe Heat Transfer Effect in Well East Mesa 6-1.

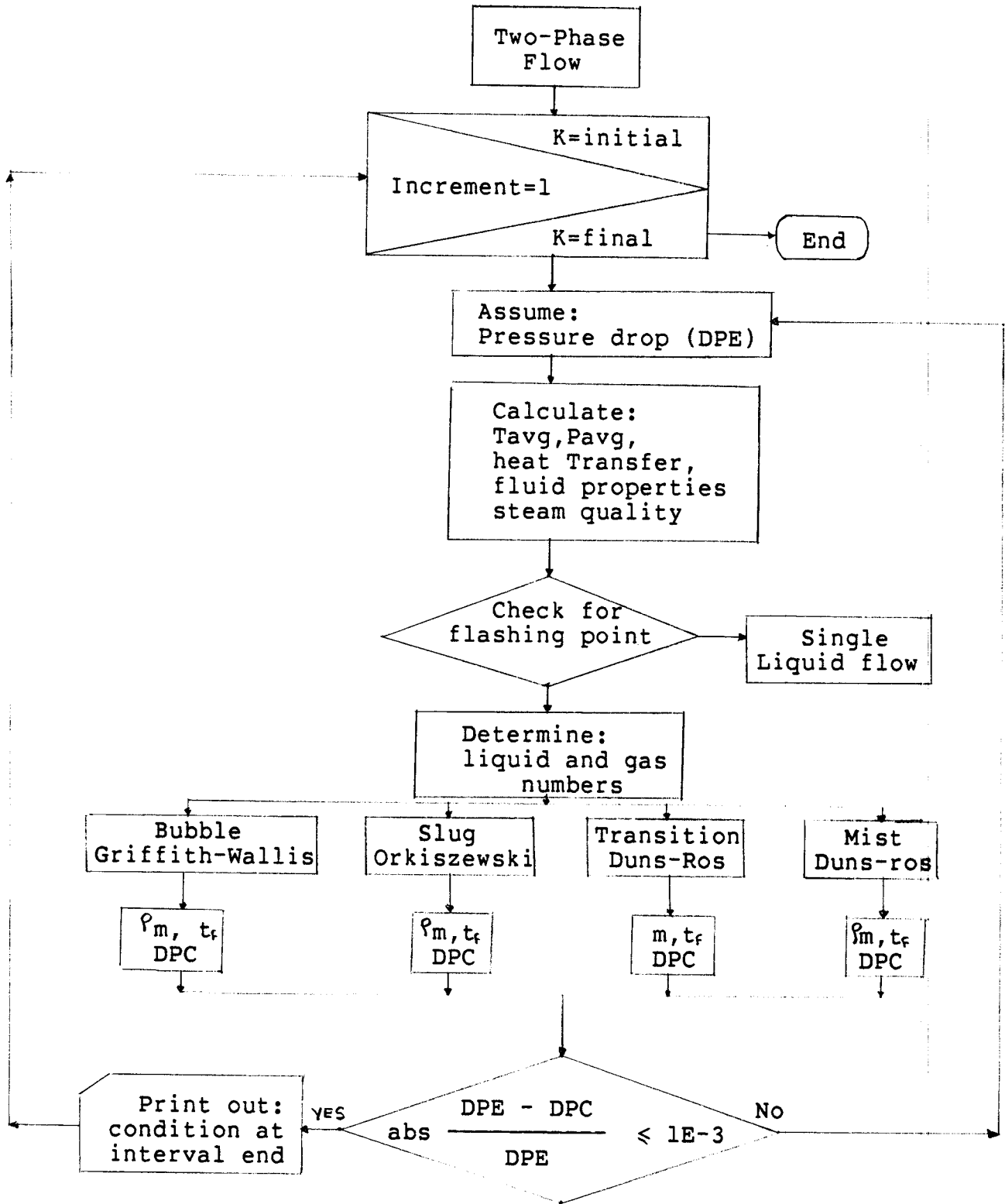
APPENDIX A

A.1 Computer Code Flow Diagram









A.2 Input Data For Two-Phase Flow Code

Card:

1. RUN FOR
2. P(1) Pressure at the initial point.....(psia) =
T(1) Temperature at the initial point.....(F) =
Z(1) Depth of initial point.....(ft) =
3. WGR Water Gravity..... =
WT Total Mass Flow Rate.....(Lb/Hr) =
ENM1 Enthalpy of mixture at initial point.(Btu/Lb) =
HCO Overall Heat Transfer Coeff...(Btu/Hr/sqft/F) =
4. INC Number of intervals..... =
5. ANG Angle of flow from the horizontal..... (Deg) =
DWELLB Depth of the wellbottom.....(ft) =
DWELLH Depth of the wellhead.....(ft) =
6. ISIGN +1 (if going down) , -1 (if going up)..... =
7. ND Number of different diameters..... =
8. DIA(1) Diameter of pipe at initial point.....(ft) =
DIA(2) Diameter of pipe at first interval..... (ft) =
DIA(3) Diameter of pipe af second interval.....(ft) =
DIA(4) Diameter of pipe at third interval..... (ft) =
9. AROG(1) Absolute roughness at initial point.....(ft) =
AROG(2) Absolute roughness first interval.....(ft) =
AROG(3) Absolute roughness second interval.....(ft) =
AROG(4) Absolute roughness third interval.....(ft) =
10. ZDIA(1) Depth of initial point.....(ft) =
ZDIA(2) Depth at which first interval ends.....(ft) =
ZDIA(3) Depth at which second interval ends.....(ft) =
ZDIA(4) Depth at which third interval ends.....(ft) =
11. NPT Number of rock temperature points..... =

12. and 13.

Depth(ft)	Rock Tem(F)	Depth(ft)	Rock Tem(F)
1	5
2	6
3	7
4	8

A.3 Computer Code Listing

```

1. //TWO PHASE JOB je.zor,TIME=(1,50)
2. // EXEC WATFIV
3. //SYSIN DD *
4. $WATFIV TIME=(0,10)
5. C *****
6. C * THIS PROGRAM CALCULATES THE FLOWING PRESSURE AND TEMPERATURE *
7. C * OF A GEOTHERMAL WELL. THE FLUID CAN EITHER BE SATURATED STEAM *
8. C * OR COMPRESSED LIQUID. THE DIRECTION OF FLOW CAN EITHER BE FROM *
9. C * THE WELLHEAD OR FROM THE BOTTOMHOLE. *
10. C * *
11. C *****
12. C * *
13. C * INPUT VARIABLES *
14. C * P(1) = FLOWING PRESSURE, PSIA *
15. C * T(1) = FLOWING TEMPERATURE, DEG. F. *
16. C * DIA = PIPE DIAMETER, FT. *
17. C * ND = NUMBER OF DIFFERENTS DIAMETERS + 1 *
18. C * ZDIAM = DEPTH OF DIFFERENTS DIAMETERS ENDINGS *
19. C * DIST = PIPE LENGTH, FT. *
20. C * AROUG = ABSOLUTE PIPE ROUGHNESS, FT. *
21. C * WGR = WATER GRAVITY *
22. C * WT = TOTAL MASS FLOW RATE, LB/HR *
23. C * ENM1 = ENTHALPY OF FLUID AT INITIAL POINT, BTU/LB *
24. C * HCO = HEAT TRANSFER COEFFICIENT, BTU/(HR.SQFT. °F) *
25. C * ENTH = ENTHALPY, BTU/LB *
26. C * ANG = ANGLE OF FLOW FROM HORIZONTAL, DEG. *
27. C * NPT = NUMBERS OF POINTS WITH SHUT-IN TEMPERATURES *
28. C * ROKT = SHUT-IN TEMPERATURE, DEG. F. *
29. C * DEPT = DEPTH OF SHUT-IN TEMPERATURE, FT. *
30. C * DWELLB = DEPTH OF WELLBORE (FT) *
31. C * DWELLH = DEPTH OF WELLHEAD (FT) *
32. C * ISIGN = +1/-1, (+1=ITERATION FROM THE WELLHEAD, *
33. C * -1=ITERATION FROM BOTTOMHOLE. ) *
34. C * *
35. C *****
36. C
37. C
38. IMPLICIT REAL*8(A-H,O-Z)
39. DIMENSION DEPT(30),ROKT(30)
40. DIMENSION P(250),T(250),Z(250),ENTH(250)
41. DIMENSION DIAM(10),ZDIAM(10),AROUG(10)
42. DIMENSION ITITLE(20),REG(5)
43. DATA REG/ 4HBBLE, 4HSLUG, 4HMIST, 4HTRAN, 4HMONO/
44. DATA IIN/5/
45. DATA IOUT/6/
46. C
47. C READ INPUT PARAMETERS
48. READ(IIN,1300)(ITITLE(I),I=1,18)
49. 1300 FORMAT(18A4)
50. READ(IIN,1000) P(1),T(1),Z(1)
51. 1000 FORMAT( 3F10.2)
52. READ(IIN,1003)WGR,WT,ENM1,HCO
53. 1003 FORMAT(4F10.2)
54. READ(IIN,4)INC
55. READ(IIN,1010) ANG,DWELLB,DWELLH
56. 1010 FORMAT(3F10.2)
57. READ(IIN,4)ISIGN
58. READ(IIN,4) ND
59. ND=ND+1
60. 4 FORMAT(I2)

```

```

61.      READ(IIN,1005) (DIAM(I),I=1,ND)
62.      1005 FORMAT(8F10.0)
63.      READ(IIN,1005)(AROU(I),I=1,ND)
64.      READ(IIN,1005) (ZDIAM(I),I=1,ND)
65.      READ (5,4) NPT
66.      READ (5,18) (DEPT(I),I=1,NPT)
67.      18 FORMAT(15F5.0)
68.      READ (5,18) (ROKT(I),I=1,NPT)
69.
70.      C
71.      WRITE(IOUT,3000)(ITITLE(I),I=1,18)
72.      3000 FORMAT(1H1,///,5X,18A4)
73.      WRITE(IOUT,3010)
74.      3010 FORMAT(//,5X,'INPUT DATA AS FOLLOW:')
75.      WRITE(IOUT,3050)WGR,WT,HCO
76.      3050 FORMAT(//,7X,'WATER GRAVITY',T35,F15.4,
77.      3 /,7X,'TOTAL MASS FLOWRATE, LB/HR',T35,F15.4,
78.      4 /,7X,'HEAT TRANSF COEFF,BTU/HR/SQFT/F',T35,F15.4)
79.      IF(ISIGN.EQ.-1) GO TO 10
80.      WRITE(IOUT,3020)
81.      3020 FORMAT(//,5X,'AT THE WELLHEAD :')
82.      WRITE(IOUT,3040)Z(1),P(1),T(1)
83.      3040 FORMAT(/,7X,'DEPTH,FT', T24,F10.2 ,
84.      1/,7X,'PRESSURE,PSIA',T24,F10.2,/ ,7X,
85.      2'TEMPERATURE,F',T24,F10.2)
86.      WRITE(IOUT,3075)
87.      3075 FORMAT(//,5X,'PIPE DIAMETER USED AS FOLLOW:',/)
88.      GO TO 11
89.      10 WRITE(IOUT,3030)
90.      3030 FORMAT(//,5X,'AT THE WELLBOTTOM:')
91.      WRITE(IOUT,3040)Z(1),P(1),T(1)
92.      WRITE(IOUT,3075)
93.      11 CONTINUE
94.      ND1 = ND-1
95.      IF(ND1.LE.0) GO TO 8
96.      DO 7 II=1,ND1
97.      WRITE(IOUT,3076)ZDIAM(II),ZDIAM(II+1),DIAM(II+1),AROU(II+1)
98.      3076 FORMAT(7X,'FROM',F8.1,' FT TO ',F8.1,' FT, PIPE DIAMETER (FT) =',
99.      1F9.4,/ ,T41,'ABS ROUGHNESS (FT) =',F9.4,/ )
100.     7 CONTINUE
101.     8 CONTINUE
102.     WRITE(IOUT,3005)INC
103.     3005 FORMAT(/,5X,'TOTAL LENGTH DIVIDED IN ',I3,' INTERVALS')
104.     WRITE(IOUT,3060)
105.     3060 FORMAT(//,5X,'DOWNHOLE SHUT-IN TEMPERATURE AS FOLLOW:',
106.     1//,7X,'DEPTH,FT',T25,'TEMP,F',/)
107.     DO 20 I=1,NPT
108.     20 WRITE(IOUT,3070)DEPT(I),ROKT(I)
109.     3070 FORMAT(2X,F12.2,5X,F10.2)
110.     WRITE(6,501)
111.     501 FORMAT(1X,/)
112.     C
113.     C CHECK FOR DENSE STATE OF GEOTHERMAL FLUID
114.     IF (T(1).GT.705.OR.P(1).GT.3208.) GO TO 100
115.     C
116.     C CONVERT ALL VARIABLES INTO ITS USABLE FORMS.
117.     SIGN = DFLOAT(ISIGN)
118.     PIE = 3.14159D0
119.     ANG = ANG*PIE/180.
120.     AROG = AROUG(1)
121.     DIA = DIAM(1)

```

```

121.         AREA = PIE*DIA*DIA/4.
122.         DIST = DWELLB-DWELLH
123.         DELZ = DIST/DFLOAT(INC)
124.         DELL = DELZ/DSIN(ANG)
125.         ISTATE = 0
126.         IONE = 1
127.         FRIMON=0.0
128.         POTMON=0.0
129.         FRITP =0.0
130.         POTTP =0.0
131.         ACCTP =0.0
132.         IPIPE = 2
133.         CENT = 0.0
134.         CENT2 = 0.0
135.         DM = 21.
136.         IF(ISIGN.EQ.1) DM=0.00
137.     C
138.     C TEST FOR COMPRESSED LIQUID
139.     PSAT=FPSAT(T(1))
140.     IF(PSAT-P(1)) 201,200,600
141.     C
142.     C * THIS IS A COMPRESSED LIQUID (SINGLE PHASE FLOW) *
143.     C
144.     201 IF (DABS(PSAT-P(1))/P(1) .LT.1.D-3) GO TO 200
145.     CALL COWAT (T(1),P(1),WDEN,ENTH1)
146.     IF (ISTATE.EQ.0) ENTH(1) = ENTH1
147.     WRITE(IOUT,3080)
148.     3080 FORMAT('1',/,10X,'* LIQUID FLOW *',
149.     1T52,'FRICTION',T64,'ACCELE.',T73,'POTENTIAL',T109,'qw/A',
150.     2/,7X,'DEPTH,FT',T18,'PRES,PSIA',T32,'TEMP,F',T40,
151.     3'EN,BTU/LB',T51,'Psi/100ft',T62,'Psi/100ft',T73,'Psi/100ft',
152.     4T109,'ft/s',/)
153.     WRITE(IOUT,3090)Z(1),P(1),T(1),ENTH(1)
154.     3090 FORMAT(4X,4(1X,F10.2),3(1X,F10.4),21X,F10.4)
155.     253 CONTINUE
156.     DPE=DELZ*0.35
157.     C
158.     C CHECK IF THIS IS THE FIRST POINT OR A TRANSFER FROM TWOPHASE.
159.     IF (ISTATE.NE.0) IONE = KFLASH
160.     IF ( ISTATE.NE.0 .AND. ISIGN.EQ.1 ) DELZ=(DWELLB-ZFLASH)/
161.     1 DFLOAT(INC-K)
162.     DELL = DELZ/DSIN(ANG)
163.     C
164.     C START TO CALCULATE PRESSURE DROP IN THE COMPRESSED LIQUID REGION.
165.     DO 30 K=IONE,INC
166.     29 ZMID = Z(K) + SIGN*DELZ/2.
167.     TR = FLAGR(DEPT,ROKT,ZMID,1,NPT)
168.     IF (ISIGN.EQ. 1.AND. ZMID.LE.ZDIAM(IPIPE)) GO TO 39
169.     IF (ISIGN.EQ.-1.AND. ZMID.GE.ZDIAM(IPIPE)) GO TO 39
170.     IPIPE = IPIPE +1
171.     AROG=AROUG(IPIPE)
172.     DIA= DIAM(IPIPE)
173.     AREA = PIE*DIA*DIA/4.
174.     39 CONTINUE
175.     C
176.     C ITERATION TO CALCULATE TEMPERATURE AND PRESSURE VALUES
177.     DO 31 I=1,500
178.     XI= DFLOAT(I-1)
179.     TAV= T(K) + SIGN*XI*.005
180.     Q = PIE*HCO*DIA*DELL*(TAV-TR)/(WT*2.)

```

```

181.          ENAV=ENTH(K) +SIGN*(Q-DELZ/1556.)
182.          IF(Q .LE. 0. ) ENAV=ENTH(K)
183.      C
184.      C      CALC. PRESSURE DROP USING THE ASSUMED FLOWING TEMPERATURE.
185.          DO 32 J=1,100
186.          PAV=P(K)+SIGN*DPE/2.
187.          CALL PVTW(TAV,PAV,WGR,DENL,VISL)
188.          ED=AROG/DIA
189.          VSL=WT/DENL/AREA/3600.
190.          REYN=1488.*DIA*VSL*DENL/VISL
191.          CALL FRFACT(REYN,ED,FM)
192.          DPDL=(FM*DENL*VSL*VSL/(32.2*2.*DIA)+DENL*DSIN(ANG))/144.
193.          DPC=DPDL*DELL
194.          IF (J .LE. 90) GO TO 4949
195.          IF (J .GT. 91) GO TO 4848
196.          WRITE(6,4747)
197.          4747 FORMAT(1X,/,1X,' J',T9,' DPE',T21,' DPC',T33,'PAV')
198.          4848 WRITE(6,1515)J,DPE,DPC,PAV
199.          1515 FORMAT(1X,I3,3(2X,F10.4))
200.          4949 CONTINUE
201.          IF (DABS(DPC-DPE).LT.0.001) GO TO 35
202.          DPE=(DPC+DPE)/2.
203.          32 CONTINUE
204.      C      SYSTEM DOES NOT CONVERGE AFTER 100 ITERATIONS
205.          WRITE (6,34)
206.          34 FORMAT (' NO CONVERGENCE AT PRESSURE ITERATION',/)
207.          GO TO 999
208.          35 CONTINUE
209.          CALL COWAT(TAV,PAV,WDEN,ENL)
210.          IF (I .LE. 400) GO TO 5050
211.          IF(I.GT.401) GO TO 5151
212.          WRITE(6,5252)
213.          5252 FORMAT(1X,/,1X,' I',T12,'ENAV',T25,'ENL',T37,'TAV')
214.          5151 WRITE(6,1616)I,ENAV,ENL,TAV
215.          1616 FORMAT(1X,I3,3(2X,F10.3))
216.          5050 CONTINUE
217.          IF (DABS(ENAV-ENL).LT..1) GO TO 36
218.          31 CONTINUE
219.      C      SYSTEM DOESN'T CONVERGE FOR 50000 P AND T ITERATIONS
220.          WRITE (6,37)
221.          37 FORMAT (' NO CONVERGENCE AT TEMPERATURE ITERATION',/)
222.          GO TO 999
223.          36 T(K+1)=T(K)+XI*SIGN*0.01
224.          P(K+1)=P(K)+DPC*SIGN
225.      C      CHECK IF FLUID IS IN SATURATED REGION
226.          PSAT=FPSAT( T(K+1) )
227.          IF( DABS(PSAT-P(K+1))/PSAT .LT. 1.D-3 ) GO TO 50
228.          IF(CENT .EQ. 1. )GO TO 45
229.          IF (P(K+1)-PSAT) 40,50,60
230.      C
231.      C      CHANGE FROM COMPRESSIBLE FLUID TO SATURATED STEAM
232.      C      WITHIN THE INCREMENT.  RECALCULATE AGAIN
233.          45 CONTINUE
234.          IF( P(K+1)-PSAT ) 42,50,46
235.          40 CONTINUE
236.          DELZ=DABS(P(K)-PSAT)/DPDL
237.          DELL=DELZ/DSIN(ANG)
238.          CENT=1.0
239.          DPE=DPDL*DELZ
240.          GO TO 29

```

```

241.          42 CONTINUE
242.          DELZ=DELZ-0.2
243.          DELL = DELZ/DSIN(ANG)
244.          GO TO 29
245.          46 CONTINUE
246.          DELZ=DELZ+0.3
247.          DELL=DELZ/DSIN(ANG)
248.          GO TO 29
249.          60 FRIT=(FM*DENL*VSL**2./(32.2*2.*DIA*144.))*DELL
250.          ACCT=0.0
251.          POTT=(DENL*DSIN(ANG)/144.)*DELZ
252.          FRIMON=FRIMON+FRIT
253.          POTMON=POTMON+POTT
254.          Z(K+1)=Z(K)+DELZ*SIGN
255.          CALL COWAT(T(K+1),P(K+1),AD,ENTH(K+1))
256.          WRITE(6,3090)Z(K+1),P(K+1),T(K+1),ENTH(K+1),
257.          1FRIT*(100./DELL),ACCT*(100./DELL),POTT*(100./DELZ),VSL
258.          30 CONTINUE
259.          WRITE(6,2626)FRIMON,POTMON,FRITP,POTTP,ACCTP
260.          GO TO 999
261.
262.          C
263.          C THIS IS THE COMPRESSED LIQUID FLASHING POINT
264.          50 Z(K+1)=Z(K)+DELZ*SIGN
265.          FRIT=(FM*DENL*VSL**2./(32.2*2.*DIA*144.))*DELL
266.          ACCT=0.0
267.          POTT=(DENL*DSIN(ANG)/144.)*DELZ
268.          FRIMON=FRIMON+FRIT
269.          POTMON=POTMON+POTT
270.          CALL COWAT (T(K+1),P(K+1),FL,FE)
271.          WRITE (6,51)
272.          51 FORMAT(/,10X,'FLASH POINT....')
273.          WRITE (6,3090) Z(K+1),P(K+1),T(K+1),FE,
274.          1FRIT*(100./DELL),ACCT*(100./DELL),POTT*(100./DELZ)
275.          KFLASH = K+1
276.          ENTH (K+1) = FE
277.          ZFLASH = Z(K+1)
278.          ISTATE =1
279.          XS=0.0
280.          C
281.          C **TWO-PHASE FLASHING FLOW**
282.          C
283.          C CHECK IF THIS IS A TRANSFER FROM COMPRESSED LIQUID REGION.
284.          200 IF (ISTATE.EQ.1) IONE = KFLASH
285.          IF(ISTATE.EQ.0) DPDL=0.009
286.          IF ( ISTATE.EQ.1 .AND. ISIGN.EQ.-1 ) DELZ=(ZFLASH-DWELLH)/
287.          1 DFLOAT(INC-K)
288.          IF (ISTATE.EQ.1) GO TO 282
289.          CALL SATUR(T(1),DENS,EHS,EHW,VISS)
290.          ENTH(1)=ENM1
291.          XS=(ENTH(1)-EHW)/(EHS-EHW)
292.          282 DELL = DELZ/DSIN(ANG)
293.          WRITE ( IOUT,2010)
294.          2010 FORMAT('1',/,10X,'* TWO-PHASE FLOW *',
295.          1T52,'FRICTION',T64,'ACCELE.',T73,'POTENTIAL',T109,'qw/A',
296.          2T119,'qs/A',/,7X,'DEPTH,FT',T18,'PRES,PSIA',T32,'TEMP,F',T40,
297.          3'EN,BTU/LB',T51,'Psi/100ft',T62,'Psi/100ft',T73,'Psi/100ft',
298.          CT85,'STM.FRAC',T97,'REGIME',T109,'ft/s',T119,'ft/s',/)
299.          C
300.          DO 210 K = IONE,INC
          IF(ISIGN.EQ.-1.AND.ISTATE.EQ.1) GO TO 254

```



```

301.         IF(K.NE.1) GO TO 254
302.         WRITE(6,5454)Z(1),P(1),T(1),ENTH(1),XS
303. 5454 FORMAT(4X,4(1X,F10.2),34X,F10.4)
304.         254 CENT1=0.0
305.         ZMID = Z(K) + SIGN*DELZ/2.
306.         TR = FLAGR (DEPT,ROKT,ZMID,1,NPT)
307.         IF (ISIGN.EQ.1 .AND. ZMID.LE.ZDIAM(IPIPE)) GO TO 69
308.         IF (ISIGN.EQ.-1 .AND. ZMID.GE.ZDIAM(IPIPE)) GO TO 69
309.         IPIPE = IPIPE + 1
310.         AROG=AROUG(IPIPE)
311.         DIA= DIAM(IPIPE)
312.         AREA = PIE*DIA*DIA/4.
313.         69 CONTINUE
314.
315. C
316. C     ITERATE TO FIND THE PRESSURE DROP
317.         DPC=DPDL*DELL
318.         DO 219 M=1,100
319.         DPE=DPC
320.         PAVG=P(K)+SIGN*(DPE/2.)
321.         TAVG=FPSAT(PAVG)
322. 550 CONTINUE
323.         Q=3.14159*HCO*DIA*(DELL/2.)*(TAVG-TR)/WT
324.         IF (TR.GE.TAVG) Q =0.0
325.         ENAV=ENTH(K)+SIGN*(Q-DELZ/2./778.)
326.         IF( Q .LE. 0. ) ENAV=ENTH(K)
327.         CALL SATUR(TAVG,DENS,ENS,ENW,VISS)
328.         X=(ENAV-ENW)/(ENS-ENW)
329.         IF ( X.LT.1. ) GO TO 202
330.         CENT1=CENT1+1.
331.         IF(CENT1.EQ.100) GO TO 220
332.         TAVG=T(K)+SIGN*CENT1*0.05
333.         PAVG=FPSAT( TAVG )
334.         DPE=2.*(PAVG-P(K))*SIGN
335.         GO TO 550
336. 202 IF ( ISTATE.EQ.1 ) GO TO 204
337.         IF (X.GT..001)GO TO 204
338.
339. C
340. C     CALCULATE THE DEPTH OF THE FLASHING POINT
341.         CENT2=1.
342.         ENAV=ENTH(K)
343.         TFP=TAVG
344.         DO 5051 N=1,200
345.         IF(N.LT.190) GO TO 9090
346.         IF(N.GT.191) GO TO 3434
347.         WRITE(6,3034)
348. 3034 FORMAT(4X,'N',T14,'TFP',T24,'ENAV',T36,'ENW',
349.         1T47,'ENS',T56,'X')
350. 3434 WRITE(6,8585)N,TFP,ENAV,ENW,ENS,X
351. 8585 FORMAT(1X,I5,4(1X,F10.3),1X,F10.4)
352. 9090 CONTINUE
353.         TFP=TFP-0.05
354.         CALL SATUR(TFP,DENS,ENS,ENW,VISS)
355.         X=(ENAV-ENW)/(ENS-ENW)
356.         IF(X.GE.-1.D-3) GO TO 5052
357. 5051 CONTINUE
358.         WRITE(6,6060)
359. 6060 FORMAT(1X,/,1X,'NO CONVERGENCE FINDING FLASH POINT')
360.         GO TO 999
361. 5052 TAVG=(T(K)+TFP)/2.
362.         PAVG=FPSAT(TAVG)

```

```

361.          CALL SATUR(TAVG,DENS,ENS,ENW,VISS)
362.          X=(ENAV-ENW)/(ENS-ENW)
363.          GO TO 204
364.      4204 CONTINUE
365.          PFP=FPSAT(TFP)
366.          Z(K+1)=Z(K)+(PFP-P(K))/DPDL
367.          P(K+1)=PFP
368.          T(K+1)=TFP
369.          CALL COWAT(TFP,PFP,DENA,ENAV)
370.          ENTH(K+1)=ENAV
371.          KFLASH = K+1
372.          ZFLASH = Z(K+1)
373.          XLEN=(Z(K+1)-Z(K))
374.          FRIT=(SDPF/144.)*XLEN
375.          ACCT=(SEKK*(DPDL))*XLEN
376.          POTT=(SDENTP*DSIN(ANG)/144.)*XLEN
377.          FRITP=FRITP+FRIT
378.          POTT=POTT+POTT
379.          ACCTP=ACCTP+ACCT
380.          WRITE(IOUT,51)
381.          WRITE (6,3090) Z(K+1),P(K+1),T(K+1),ENAV,
382.          1FRIT*(100./XLEN),ACCT*(100./XLEN),POTT*(100./XLEN)
383.          WRITE(6,3080)
384.          ISTATE = 1
385.          GO TO 253
386.      C
387.      204 CALL PVTW(TAVG,PAVG,WGR,DENW,VISW)
388.          SUR=FSURW( TAVG,PAVG )
389.          WS = X*WT
390.          WW=WT-WS
391.          VSW=WW/DENW/AREA/3600.
392.          VSS=WS/DENS/AREA/3600.
393.          HLNS=VSW/(VSW+VSS)
394.          VM=VSW+VSS
395.          XGN=1.938*VSS*((DENW/SUR)**0.25)
396.          XLN=1.938*VSW*((DENW/SUR)**0.25)
397.      C
398.          CALL ORKIS(HLNS,XLN,XGN,ANG,DENW,DENS,VM,DIA,VSS,VSW,
399.          1PAVG,AROG,VISW,VISS,SUR,HL,DPDL,IFP,SDPF,SEKK,
400.          2SDENTP,XBL,XSL,XML,SIG,DM)
401.          IF(ISIGN.EQ.-1) DM=SDENTP
402.          DPDL=-DPDL
403.          DPC=DELL*DPDL
404.          IF(M.LT.50) GO TO 1818
405.          IF(M.GE.51) GO TO 8181
406.          WRITE(6,7171)
407.          7171 FORMAT(/,1X,' M',T7,' DPE',T14,' DPC',T22,'TAVG',T29,
408.          1'ENAV',T38,'X',T42,'VSW',T48,'VSS',T52,'HLNS',T59,
409.          2'HL',T63,'DENW',T69,'DENS',T76,'XLN',T82,'XGN',T87,
410.          3'VISW',T93,'SDPF',T98,'SEKK',T103,'SDENTP',T109,'IFP',T112,
411.          4'XBL',T117,'XSL',T122,'XML',T129,'SIG')
412.          8181 WRITE(6,2121)M,DPE,DPC,TAVG,ENAV,X,VSW,VSS,
413.          1HLNS,HL,DENW,DENS,XLN,XGN,VISW,SDPF,SEKK,SDENTP,IFP,XBL,
414.          2XSL,XML,SIG
415.          2121 FORMAT(1X,I3,2F7.3,2F7.2,F6.3,2F6.2,2F5.2,2F6.2,2F6.1,
416.          1F6.3,F6.2,F5.2,F7.3,I2,F4.1,2F5.0,F8.4)
417.          1818 CONTINUE
418.          IF(CENT2.EQ.1.) GO TO 4204
419.          IF (DABS(DPE-DPC)/DPE.LT.1.D-3) GO TO 130
420.          219 CONTINUE

```

```

421.      220 CONTINUE
422.      C      SYSTEM DOES NOT CONVERGES AFTER 100 ITERATIONS.
423.      WRITE(IOUT,1111)CENT1,DPE-DPC
424.      1111 FORMAT(5X,'cent1 ',F5.0,1X,'DIFFE ',F10.3)
425.      WRITE (6,221) Z(K),P(K),T(K)
426.      221 FORMAT (' TWO-PHASE FLASHING FLOW',/,
427.      C' NO CONVERGENCE AT DEPTH= ',F10.3,' PRESSURE= ',
428.      CF10.3,' TEMPERATURE= ',F10.3)
429.      GO TO 999
430.      C
431.      130 CONTINUE
432.      FRIT=(SDPF/144.)*DELL
433.      ACCT=(SEKK*(DPDL))*DELL
434.      POTT=(SDENTP*DSIN(ANG)/144.)*DELL
435.      FRITP=FRITP+FRIT
436.      POTT= POTT+POTT
437.      ACCTP=ACCTP+ACCT
438.      ENTH(K+1)=ENTH(K) + DABS(ENTH(K)-ENAV)*2*SIGN
439.      Z(K+1)=Z(K)+DELZ*SIGN
440.      P(K+1)= P(K) + SIGN*DPC
441.      T(K+1)=FTSAT(P(K+1))
442.      CALL SATUR(T(K+1),DENS,ENS,ENW,VISS)
443.      X=(ENTH(K+1)-ENW)/(ENS-ENW)
444.      111 WRITE(IOUT,2000) Z(K+1), P(K+1),T(K+1),ENTH(K+1),
445.      1FRIT*(100./DELL),ACCT*(100./DELL),POTT*(100./DELL),
446.      2X,REG(IFP),VSW,VSS
447.      2000 FORMAT(4X,4(1X,F10.2),4(1X,F10.4),T99,A4,2F10.4)
448.      210 CONTINUE
449.      WRITE(6,2626)FRIMON,POTMON,FRITP,POTT,ACCTP
450.      2626 FORMAT(///,T30,'** PRESSURE ANALYSIS **',/,
451.      C /,25X,'TOTAL FRICTION, LIQUID      =',F10.4,' PSI',
452.      1 /,25X,'TOTAL POTENTIAL, LIQUID      =',F10.4,' PSI',
453.      2//,25X,'TOTAL FRICTION, TWO-PHASE    =',F10.4,' PSI',
454.      3 /,25X,'TOTAL POTENTIAL, TWO-PHASE   =',F10.4,' PSI',
455.      4 /,25X,'TOTAL ACCELE., TWO-PHASE    =',F10.4,' PSI')
456.      GO TO 999
457.      C
458.      600 IF ((PSAT-P(1))/P(1)).LT.1.D-3) GO TO 200
459.      WRITE(IOUT,2020)
460.      2020 FORMAT(///,15X,'SUPER HEATED STEAM, RUN TERMINATED',/)
461.      TSAT=FTSAT(P(1))
462.      WRITE(6,8899) P(1),TSAT
463.      8899 FORMAT(1X,'FOR ',F10.2,' TEMP SAT = ',F10.2)
464.      GO TO 999
465.      100 WRITE (6,2040)
466.      2040 FORMAT (' PRESSURE OR TEMPERATURE IS ABOVE CRITICAL POINT
467.      1: PROGRAM EXECUTION IS TERMINATED ')
468.      999 CONTINUE
469.      WRITE(IOUT,2001)
470.      2001 FORMAT(1X,/)
471.      STOP
472.      END
473.      C
474.      C
475.      SUBROUTINE ORKIS(HLNS,XLN,XGN,ANG,DL,DG,VM,D,VSG,VSL,
476.      1P,RTUB,VL,VG,SUR,HL,DPDL,IREG,DPF,EKK,DENTP,
477.      2XBL,XSL,XML,SIG,DM)
478.      IMPLICIT REAL*8(A-H,O-Z)
479.      REL=1488.*DL*VM*D/VL
480.      KOUNT=1

```

```

481.          CENT3=1.
482.          FAC=2.*32.2*D
483.          REG=1488.*DG*VSG*D/VG
484.          ED=RTUB/D
485.      C      CHECK FOR SINGLE PHASE FLOW
486.          IF(VSG.LT..00001)GO TO 2500
487.          IF(VSL.LT..00001)GO TO 2600
488.          XBL1=1.02355+1.47463*XLN-0.174706D-1*XLN**2.
489.          XBL2=.108803D-2*XLN**3.-0.139331D-4*XLN**4.
490.          XBL=XBL1+XBL2
491.          XSL=50.+36.*XLN
492.          XML=75.+84.*XLN**.75
493.          IF(XGN .LT. 0.1) GO TO 2500
494.          IF(XGN .LT. XBL) GO TO 1
495.          IF(XGN .LT. XSL) GO TO 4
496.          IF(XGN .LT. XML) KOUNT=2
497.          IF(XGN .LT. XML) GO TO 4
498.          IF(XGN .GT. XML) GO TO 5
499.      C
500.      C      BUBBLE FLOW CALCULATIONS
501.          1 VS=.8
502.          HL=1.-.5*(1.+VM/V5-DSQRT(((1.+VM/V5)**2-4.*VSG/V5))
503.          IF(HL.LT.HLNS)HL=HLNS
504.          RELB=1488.*DL*VSL*D/HL/VL
505.          CALL FRFACT(RELB,ED,FF)
506.          DPF=FF*DL*VSL*VSL/HL/HL/FAC
507.          EKK=0.
508.          DENTP=DL*HL*DG*(1.-HL)
509.          IREG=1
510.          GO TO 2000
511.      C
512.      C      SLUG FLOW CALCULATIONS
513.          4 SIG=.045*DLOG10(VL)/D**.799-.709-.162*DLOG10(VM)-.888*DLOG10(D)
514.          TLI=-0.065*VM-0.1
515.      CC      WRITE(6,1312)SIG,TLI
516.      CC 1312 FORMAT(1X,2F10.4)
517.          IF(SIG.LT.TLI) SIG=TLI
518.      C      ITERATING FOR VB
519.          VB1=.5*DSQRT(32.2*D)
520.          I=0
521.          10 REB=1488.*DL*VB1*D/VL
522.          I=I+1
523.          IF(I.GT.10)GO TO 12
524.          XX=DSQRT(32.2*D)
525.          TX=(.251+8.74D-06*REL)*XX
526.          VB=TX/2.+DSQRT(TX*TX+(13.59*VL)/(DL*DSQRT(D)))
527.          IF(REB.LE.3000.)VB=(.546+8.74D-06*REL)*XX
528.          IF(REB.GE.8000.)VB=(.35+8.74D-06*REL)*XX
529.      CC      WRITE(6,1212)I,II,REL,REB,VB1,VB,SIG
530.      CC 1212 FORMAT(1X,2I2,2F10.0,3F10.4)
531.          11 IF(DABS(VB-VB1).LT..001)GO TO 12
532.          VB1=VB
533.          GO TO 10
534.          12 CONTINUE
535.          DENTP=(DL*(VSL+VB)+DG*VSG)/(VM+VB)+DL*SIG
536.          IF(SIG.EQ.TLI.AND.CENT3.EQ.1.) GO TO 13
537.          IF(CENT3.EQ.1..AND.DM.NE.0.0) DENTP=DM
538.          TLI=-VB*(1.-DENTP/DL)/(VM+VB)
539.          CENT3=CENT3+1.
540.      CC      IF(CENT3.GT.2.) GO TO 1414

```

```

541.      CC      WRITE(6,1213)DENTP,SIG,TLI
542.      CC 1213 FORMAT(1X,3F10.4)
543.      CC 1414 CONTINUE
544.          IF((SIG-TLI).GT.-1.D-5) GO TO 13
545.          SIG=TLI
546.          GO TO 12
547.      13 CONTINUE
548.          HL=(DENTP-DG)/(DL-DG)
549.          CALL FRFACT(REL,ED,FF)
550.          XX=FF*DL*VM*VM/FAC
551.          DPF=XX*((VSL+VB)/(VM+VB)+SIG)
552.          EKK=0.
553.          IREG=2
554.          IF(KOUNT.EQ.2)GO TO 51
555.          GO TO 2000
556.      C
557.      C      MIST FLOW CALCULATIONS
558.          5 KUNT=1
559.          VSGP=VSG
560.          80 REYG=1488.*DG*VSGP*D/VG
561.          XWEB=454.*DG*VSGP*VSGP*ED/SUR
562.          XWEV=.0002048D0*VL*VL/DL/SUR/(ED*D)
563.          PR=XWEB*XWEV
564.          ED=.0749*SUR/DG/VSGP/VSGP/D
565.          IF(PR.GT..005)FD=.0385*SUR*PR**.302/DG/VSGP/VSGP/D
566.          VSGP=VSG/(1.-ED)/(1.-ED)
567.          IF(KUNT.GT.1)GO TO 60
568.          KUNT=3
569.          GO TO 80
570.          60 IF(ED.LT..05)GO TO 70
571.          FF=1./(4.*DLOG10(.27*ED))**2+.067*ED**1.73
572.          GO TO 90
573.          70 CALL FRFACT(REYG,ED,FF)
574.          90 DPF=FF*DG*VSGP*VSGP/FAC
575.          DENTP=DL*HLNS+DG*(1.-HLNS)
576.          HL=HLNS
577.          EKK=VSGP*VM*DENTP/P/32.2/144.
578.          IF(EKK.GT..95)EKK=.95
579.          IREG=3
580.          IF(KOUNT.EQ.2)GO TO 52
581.          GO TO 2000
582.      C
583.      C      CALCULATIONS FOR THE TRANSITION REGION
584.          51 DPS=-(DPF+DENTP*DSIN(ANG))/144.
585.          DENMS=DENTP
586.          DPFS=DPF
587.          GO TO 5
588.          52 DPM=-(DPF+DENTP*DSIN(ANG)*XGN/XML)/144./(1.-EKK)
589.          DENMM=DENTP*(XGN/XML)
590.          DPFM=DPF
591.          A=(XML-XGN)/(XML-XSL)
592.          B=(XGN-XSL)/(XML-XSL)
593.          DENTP=DENMS*A+DENMM*B
594.          DPF=DPFS*A+DPFM*B
595.      CC      WRITE(6,5252)A,B,DPS,DPM,DPFS,DPFM,DENMS,DENMM
596.      CC 5252 FORMAT(1X,8(1X,F10.3))
597.          DPDL=A*DPS+B*DPM
598.          IREG=4
599.          GO TO 3000
600.      C

```

```

601.      C      FOR SINGLE PHASE LIQUID
602.      2500 CALL FRFACT(REL,ED,FF)
603.          DENTP=DL
604.          EKK=0.
605.          HL=HLNS
606.          IREG=5
607.          DPF=FF*DL*VSL*VSL/FAC
608.          GO TO 2000
609.      2600 CALL FRFACT(REG,ED,FF)
610.          EKK=0.
611.          DENTP=DG
612.          DPF=FF*DG*VSG*VSG/FAC
613.          IREG=3
614.      2000 DPDL=-(DPF+DENTP*DSIN(ANG))/144./(1.-EKK)
615.      3000 CONTINUE
616.          RETURN
617.          END
618.
619.      C
620.          SUBROUTINE FRFACT( REY,ED,FF)
621.          IMPLICIT REAL*8(A-H,O-Z)
622.          FF1 = 64./REY
623.          FGI = .0056+.5/REY**.32
624.          I=1
625.      5 DEN=1.14-2.*DLOG10(ED+9.34/(REY*DSQRT(FGI)))
626.          FF =(1./DEN)**2
627.          DIFF=DABS(FGI-FF)
628.          IF(DIFF-.0001)8,8,6
629.      6 FGI=(FGI+FF)/2.
630.          I = I+1
631.          IF (I-10) 5,5,7
632.      7 FF=FGI
633.          8 IF(FF-FF1)9,10,10
634.          9 FF=FF1
635.      10 RETURN
636.          END
637.
638.      C
639.          SUBROUTINE COWAT(TF,PP,DENL,EBP)
640.          IMPLICIT REAL*8(A-H,O-Z)
641.          DIMENSION A(23),SA(12)
642.          DATA A/
643.      16.824687741D3,-5.422063673D2,-2.096666205D4,3.941286787D4,
644.      2-6.733277739D4,9.902381028D4,-1.093911774D5,8.590841667D4,
645.      3-4.511168742D4,1.418138926D4,-2.017271113D3,7.982692717D0,
646.      4-2.616571843D-2,1.522411790D-3,2.284279054D-2,2.421647003D2,
647.      51.269716088D-10,2.074838328D-7,2.174020350D-8,1.105710498D-9,
648.      61.293441934D1,1.308119072D-5,6.047626338D-14/
649.          DATA SA/
650.      18.438375405D-1,5.362162162D-4,1.720000000D0,7.342278489D-2,
651.      24.975858870D-2,6.537154300D-1,1.150D-6,1.51080D-5,
652.      31.41880D-1,7.002753165D0,2.995284926D-4,2.040D-1 /
653.          TC=((TF+40.)/1.8)-40.
654.          TKR=(TC+273.15)/647.3
655.          PBAR=PP/14.5038
656.          PNMN=PBAR/2.212D2
657.          Y=1.-SA(1)*TKR*TKR-SA(2)/TKR**6
658.          Z=Y+(SA(3)*Y*Y-2.*SA(4)*TKR+2.*SA(5)*PNMN)**.5
659.          DENL=0.0
660.          YD=-2.*SA(1)*TKR+6.*SA(2)/TKR**7
661.          SNUM=0.
662.          DO 10 I=1,10

```

```

661.      10 SNUM=SNUM+(I-2)*A(I+1)*TKR**(I-1)
662.      PRT1=A(12)*(Z*(17.*(Z/29.-Y/12.))+5.*TKR*YD/12.)+SA(4)*TKR-
663.      1(SA(3)-1.)*TKR*Y*YD)/Z**(5./17.)
664.      PRT2=PNMR*(A(13)-A(15)*TKR*TKR+A(16)*(9.*TKR+SA(6))*(SA(6)-TKR)**9
665.      2+A(17)*(20.*TKR**19+SA(7)))/(SA(7)+TKR**19)**2)
666.      PRT3=(12.*TKR**11+SA(8))/(SA(8)+TKR**11)**2*(A(18)*PNMR+A(19)*
667.      3PNMR*PNMR+A(20)*PNMR*PNMR*PNMR)
668.      PRT4=A(21)*TKR**18*(17.*SA(9)+19.*TKR*TKR)*(1./(SA(10)+PNMR)**3+
669.      4SA(11)*PNMR)
670.      PRT5=A(22)*SA(12)*PNMR**3+21.*A(23)/TKR**20*PNMR**4
671.      ENTR=A(1)*TKR-SNUM+PRT1+PRT2-PRT3+PRT4+PRT5
672.      EJG=ENTR*70.1204D0
673.      EBP=EJG*429.923D-3
674.      RETURN
675.      END
676.
677.      C
678.      FUNCTION FLAGR(X,Y,XARG,IDEG,NPTS)
679.      IMPLICIT REAL*8(A-H,O-Z)
680.      DIMENSION X(1),Y(1)
681.      N=NPTS
682.      N1=IDEG+1
683.      L=1
684.      IF(NPTS.LT.0)L=2
685.      IF(NPTS.LT.0)N=-N
686.      GO TO (10,20),L
687.      10 DO 11 MAX =N1,N
688.      IF(XARG.LT.X(MAX)) GO TO 12
689.      11 CONTINUE
690.      MAX=N
691.      GO TO 12
692.      20 DO 21 MAX=N1,N
693.      IF(XARG.GT.X(MAX)) GO TO 12
694.      21 CONTINUE
695.      MAX=N
696.      12 MIN=MAX-IDEG
697.      FACTOR=1.
698.      DO 2 I=MIN,MAX
699.      IF(XARG.NE.X(I)) GO TO 2
700.      FLAGR=Y(I)
701.      RETURN
702.      2 FACTOR=FACTOR*(XARG-X(I))
703.      YEST=0.
704.      DO 5 I=MIN,MAX
705.      TERM=Y(I)*FACTOR/(XARG-X(I))
706.      DO 4 J=MIN,MAX
707.      4 IF(I.NE.J) TERM=TERM/(X(I)-X(J))
708.      5 YEST=YEST+TERM
709.      FLAGR=YEST
710.      RETURN
711.      END
712.
713.      C
714.      FUNCTION FPSAT(TF)
715.      IMPLICIT REAL * 8 (A-H,O-Z)
716.      REAL * 8 XK(9)
717.      DATA XK/-.691234564,-2.608023696D1,-1.681706546D2,6.423285504D1,
718.      1-1.189646225D2,4.167117320D0,2.097506760D1,1.D9,6.D0/
719.      TC=((TF+40.)/1.8)-40.
720.      TKR=(TC+273.15)/647.3
721.      TKRM=1.-TKR
722.      SUM=0.

```

```

721.      DO 10 I=1,5
722.      10 SUM=SUM+XK(I)*TKRM**I
723.      DENO=1.+XK(6)*TKRM+XK(7)*TKRM*TKRM
724.      CONS=TKRM/(XK(8)*TKRM*TKRM+XK(9))
725.      PNMIR=DEXP((1./TKR)*SUM/DENO-CONS)
726.      PBAR=PNMIR*2.212D2
727.      PPSI=PBAR*14.5038
728.      FPSAT=PPSI
729.      RETURN
730.      END
731.      C
732.      FUNCTION FTSAT(P)
733.      IMPLICIT REAL * 8 (A-H,O-Z)
734.      T=116.845*P**0.22302
735.      DO 17 I=1,200
736.      PCA=FPSAT(T)
737.      XSIG=-1.0
738.      IF((PCA-P).LT.0.) XSIG=1.
739.      IF(DABS(PCA-P)/P .LT. 1D-3) GO TO 43
740.      T=T+XSIG*.03
741.      17 CONTINUE
742.      43 FTSAT=T
743.      RETURN
744.      END
745.      C
746.      SUBROUTINE SATUR(TF,DES,EHS,EHW,VIS)
747.      IMPLICIT REAL*8(A-H,O-Z)
748.      DIMENSION TD(33),XVS(33),XES(33),XEW(33)
749.      DIMENSION XVW(33)
750.      C
751.      DATA XVW/1.0121D0,1.0171D0,1.0228D0,1.0290D0,1.0359D0,1.0435D0,
752.      C1.0515D0,1.0603D0,
753.      O1.0679D0,1.0798D0,1.0906D0,1.1021D0,1.1144D0,1.1275D0,1.1415D0,
754.      C1.1565D0,1.1726D0,
755.      P1.1900D0,1.2087D0,1.2291D0,1.2512D0,1.2755D0,1.3023D0,1.3321D0,
756.      C1.3655D0,1.4036D0,
757.      Q1.4475D0,1.4992D0,1.5620D0,1.6390D0,1.7410D0,1.8940D0,2.220D0/
758.      DATA TD/50.0D0,60.0D0,70.0D0,80.0D0,90.0D0,100.0D0,110.0D0,120.0D0,
759.      C130.0D0,140.0D0,150.0D0,160.0D0,
760.      2170.0D0,180.0D0,190.0D0,200.0D0,210.0D0,220.0D0,230.0D0,240.0D0,250.0D0,
761.      C260.0D0,270.0D0,280.0D0,290.0D0,
762.      3300.0D0,310.0D0,320.0D0,330.0D0,340.0D0,350.0D0,360.0D0,370.0D0/
763.      DATA XVS/12045.0D0,7677.6D0,5045.3D0,3408.3D0,2360.9D0,
764.      C1673.0D0,1210.1D0,891.71D0,
765.      4668.32D0,508.66D0,392.57D0,306.85D0,242.62D0,193.85D0,
766.      C156.35D0,127.19D0,104.265D0,
767.      586.062D0,71.472D0,59.674D0,50.056D0,42.149D0,35.599D0,
768.      C30.133D0,25.537D0,21.643D0,
769.      618.316D0,15.451D0,12.967D0,10.779D0,8.805D0,6.943D0,4.93D0/
770.      DATA XES/2592.0D0,2609.0D0,2626.0D0,2643.0D0,2660.0D0,2676.0D0,
771.      C2691.0D0,2706.0D0,2720.0D0,
772.      72734.0D0,2747.0D0,2758.0D0,2769.0D0,2778.0D0,2786.0D0,2793.0D0,
773.      C2798.0D0,2802.0D0,2803.0D0,2803.0D0,
774.      82801.0D0,2796.0D0,2790.0D0,2780.0D0,2766.0D0,2749.0D0,2727.0D0,
775.      C2700.0D0,2666.0D0,2623.0D0,2565.0D0,
776.      92481.0D0,2331.0D0/
777.      DATA XEW/209.3D0,251.1D0,293.0D0,334.9D0,376.9D0,419.1D0,
778.      C461.3D0,503.7D0,546.3D0,
779.      X589.1D0,632.2D0,675.5D0,719.1D0,763.1D0,807.5D0,852.4D0,
780.      C897.7D0,943.7D0,990.3D0,

```



```

781.      Y1037.6D0,1085.8D0,1135.0D0,1185.2D0,1236.8D0,1290.D0,
782.      C1345.D0,1402.D0,1462.D0,
783.      Z1526.D0,1596.D0,1672.D0,1762.D0,1892.D0/
784.      TC=((TF+40.)/1.8)-40.
785.      C
786.      XDS=FLAGR(TD,XVS,TC,2,33)
787.      DES=1./XDS*62.428
788.      XHS=FLAGR(TD,XES,TC,2,33)
789.      EHS=XHS*1000./2324.4
790.      XHW=FLAGR(TD,XEW,TC,2,33)
791.      EHW=XHW*1000./2324.4
792.      VTS=.407*TC+80.4-(1858.-5.9*TC)/XDS
793.      VIS=VTS/10000.
794.      C
795.      C      XDW=FLAGR(TD,XVW,TC,2,33)
796.      C      DEW=1./XDW*62.428
797.      RETURN
798.      END
799.      C
800.      FUNCTION FSURW(TF,PP)
801.      IMPLICIT REAL*8(A-H,O-Z)
802.      DIMENSION STVA(10),STV74(10),STV280(10)
803.      DATA STVA/
804.      10.D0,1000.D0,2000.D0,3000.D0,4000.D0,5000.D0,
805.      C6000.D0,7000.D0,8000.D0,9000.D0/
806.      DATA STV74/
807.      275.D0,63.D0,59.D0,57.D0,54.D0,52.D0,52.D0,51.D0,50.D0,49.D0/
808.      DATA STV280/
809.      353.D0,46.D0,40.D0,33.D0,26.D0,21.D0,21.D0,22.D0,23.D0,24.D0/
810.      TEM1=TF
811.      P=PP
812.      STW74=FLAGR(STVA,STV74,P,2,10)
813.      STW280=FLAGR(STVA,STV280,P,2,10)
814.      STW=(STW74-STW280)/(280.-74.)*(TEM1-74.)*(-1.)+STW74
815.      IF(TEM1.LT.74.)STW=STW74
816.      IF(TEM1.GT.280.)STW=STW280
817.      SURW=STW
818.      FSURW=SURW
819.      RETURN
820.      END
821.      C
822.      SUBROUTINE PVTW(TF,PP,SGW,DEN,VIS)
823.      IMPLICIT REAL*8(A-H,O-Z)
824.      TA=TF-60.D0
825.      BW=1.D0+1.2D-4*TA+1.D-6*TA*TA-3.33D-6*PP
826.      DEN=62.43D0*SGW/BW
827.      VIS=DEXP(1.003D0-1.479D-2*TF+1.982D-5*TF*TF)
828.      RETURN
829.      END
830.      $DATA
831.      RUN FOR CERRO PRIETO M-90, 21/FEB/78
832.      0590.00  484.3  0000.0
833.      1.0190  356840.00  577.44  00.00
834.      43
835.      90.      4260.7  0.0
836.      +1
837.      01
838.      .5808    .5808
839.      .0003    .0003
840.      0.0000  4260.7
841.      05
842.      0000.2297.3281.3937.4518.
843.      0077.0102.0294.0557.567.9
844.      $STOP

```

A.4 Typical Output of the Computer Code

RUN FOR CERRO PRIETO H-90, 21/FEB/78

INPUT DATA AS FOLLO:

WATER GRAVITY 1.0190
 TOTAL MASS FLOWRATE, LB/HR 356840.0000
 HEAT TRANSF COEFF, BTU/HR/SQFT/F 0.0000

AT THE WELLHEAD :

DEPTH, FT 0.00
 PRESSURE, PSIA 590.00
 TEMPERATURE, F 484.30

PIPE DIAMETER USED AS FOLLO:

FROM 0.0 FT TO 4260.7 FT, PIPE DIAMETER (FT) = 0.5808
 ABS ROUGHNESS (FT) = 0.0003

TOTAL LENGTH DIVIDED IN 43 INTERVALS

WELLBORE SHUT-IN TEMPERATURE AS FOLLO:

DEPTH, FT	TEMP, F
0.00	77.00
2297.00	102.00
3281.00	294.00
3937.00	557.00
4516.00	567.90

* TWO-PHASE FLOW *		TEMP, F	EN, BTU/LB	FRICTION Psi/100ft	ACCELE. Psi/100ft	POTENTIAL Psi/100ft	STH. FRAC	REGIME	qm/A ft/s	qa/A ft/s
DEPTH, FT	PRES. PSIA									
0.00	590.00	484.30	577.44				0.1464			
99.09	600.83	486.44	577.44	5.5482	0.0000	5.3862	0.1435	SLUG	6.1863	42.0231
198.17	611.67	488.36	577.44	5.3762	0.0000	5.5606	0.1410	SLUG	6.2148	40.4845
297.26	622.52	490.28	577.44	5.2133	0.0000	5.7363	0.1383	SLUG	6.2428	39.0271
396.34	633.39	492.15	577.44	5.0541	0.0000	5.9191	0.1358	SLUG	6.2711	37.6016
495.43	644.30	494.03	577.44	4.9032	0.0000	6.1036	0.1332	SLUG	6.2988	36.2489
594.52	655.25	495.86	577.44	4.7552	0.0000	6.2904	0.1280	SLUG	6.3270	34.9218
693.60	666.25	497.70	577.44	4.6145	0.0000	6.4804	0.1256	SLUG	6.3547	33.6597
792.69	677.32	499.51	577.44	4.4763	0.0000	6.6835	0.1228	SLUG	6.3829	32.4183
891.77	688.46	501.33	577.44	4.3443	0.0000	6.8996	0.1203	SLUG	6.4107	31.2310
990.86	699.69	503.11	577.44	4.2127	0.0000	7.1182	0.1176	SLUG	6.4391	30.0884
1089.95	711.01	504.92	577.44	4.0866	0.0000	7.3401	0.1150	SLUG	6.4672	28.9161
1189.03	722.44	506.72	577.44	3.9621	0.0000	7.5742	0.1123	SLUG	6.4958	27.7947
1288.12	733.99	508.49	577.44	3.8429	0.0000	7.8129	0.1097	SLUG	6.5242	26.7196
1387.20	745.67	510.28	577.44	3.7246	0.0000	8.0648	0.1069	SLUG	6.5533	25.6528
1486.29	757.50	512.08	577.44	3.6093	0.0000	8.3267	0.1043	SLUG	6.5826	24.6110
1585.38	769.48	513.85	577.44	3.4985	0.0000	8.5998	0.1015	SLUG	6.6117	23.6096
1684.46	781.64	515.65	577.44	3.3882	0.0000	8.8785	0.0987	SLUG	6.6416	22.6132
1783.55	793.98	517.43	577.44	3.2805	0.0000	9.1752	0.0959	SLUG	6.6718	21.6376
1882.63	806.52	519.24	577.44	3.1766	0.0000	9.4808	0.0930	SLUG	6.7019	20.6956
1981.72	819.29	521.06	577.44	3.0722	0.0000	9.8091	0.0901	SLUG	6.7330	19.7480
2080.81	832.29	522.90	577.44	2.9696	0.0000	10.1545	0.0872	SLUG	6.7645	18.8160
2179.89	845.55	524.72	577.44	2.8703	0.0000	10.5126	0.0841	SLUG	6.7961	17.9134
2278.98	859.09	526.58	577.44	2.7709	0.0000	10.8960	0.0810	SLUG	6.8287	17.0093
2378.07	872.94	528.46	577.44	2.6731	0.0000	11.3041	0.0779	SLUG	6.8629	16.1175
2477.15	887.12	530.37	577.44	2.5767	0.0000	11.7366	0.0747	SLUG	6.8960	15.2370
2576.24	901.66	532.27	577.44	2.4830	0.0000	12.1897	0.0713	SLUG	6.9303	14.3804
2675.32	916.60	534.22	577.44	2.3889	0.0000	12.6611	0.0679	SLUG	6.9659	13.5193
2774.41	931.96	536.21	577.44	2.2958	0.0000	13.2073	0.0644	SLUG	7.0024	12.6664
2873.50	947.79	538.23	577.44	2.2032	0.0000	13.7765	0.0608	SLUG	7.0400	11.8164
2972.59	964.15	540.26	577.44	2.1110	0.0000	14.3942	0.0568	SLUG	7.0787	10.9688
3071.67	983.83	542.70	577.44	4.3751	0.0000	15.4883	0.0565	BBLE	7.1215	10.0680
3170.75	1003.92	545.16	577.44	3.9149	0.0000	16.3659	0.0520	BBLE	7.1693	9.1025
3269.84	1024.55	547.64	577.44	3.4919	0.0000	17.3219	0.0474	BBLE	7.2182	8.1572
3368.93	1045.82	550.16	577.44	3.1020	0.0000	18.3720	0.0427	BBLE	7.2685	7.2271
3468.01	1067.90	552.73	577.44	2.7420	0.0000	19.5355	0.0378	BBLE	7.3205	6.3074
3567.10	1090.93	555.37	577.44	2.4092	0.0000	20.8376	0.0327	BBLE	7.3747	5.3932
3666.18	1115.13	558.10	577.44	2.0995	0.0000	22.3202	0.0273	BBLE	7.4315	4.4747
3765.27	1140.71	560.90	577.44	1.8160	0.0000	24.0007	0.0216	BBLE	7.4908	3.5517
3864.36	1167.98	563.87	577.44	1.5510	0.0000	25.9741	0.0155	BBLE	7.5546	2.6286
3963.44	1197.33	567.00	577.44	1.3067	0.0000	28.3141	0.0089	BBLE	7.6231	1.6789
4062.53	1229.26	570.34	577.44	1.0823	0.0000	31.1366	0.0017	BBLE	7.6974	0.7049
FLASH POINT....										
4098.33	1241.59	571.52	577.63	0.9351	0.0000	33.5126				
* LIQUID FLOW *		TEMP, F	EN, BTU/LB	FRICTION Psi/100ft	ACCELE. Psi/100ft	POTENTIAL Psi/100ft			qm/A ft/s	
DEPTH, FT	PRES. PSIA									
4260.70	1297.50	571.53	577.44	0.9365	0.0000	33.4982		7.7561		

** PRESSURE ANALYSIS **

TOTAL FRICTION, LIQUID = 1.8207 PSI
 TOTAL POTENTIAL, LIQUID = 54.3926 PSI
 TOTAL FRICTION, TWO-PHASE = 136.4520 PSI
 TOTAL POTENTIAL, TWO-PHASE = 515.1387 PSI
 TOTAL ACCELE., TWO-PHASE = 0.0000 PSI

STATEMENTS EXECUTED= 146607
 CORE USAGE OBJECT CODE= 43528 BYTES, ARRAY AREA= 10784 BYTES, TOTAL AREA AVAILABLE= 221184 BYTES
 DIAGNOSTICS NUMBER OF ERRORS= 0, NUMBER OF WARNINGS= 0, NUMBER OF EXTENSIONS= 15

APPENDIX B

Table B.1 East Mesa 6-1

Flowing Profile			Shut-in Profile
Depth ft	Pressure psia	Temperature F	Temperature F
7000	1348.03	389.3	381.2
6000	961.	389.	369.3
5500	767	388.	365.0
5000	574	387.	360.2
4500	381	386	356.0
4050	208	385.	-
4000	192	377.	350.6
3500	115	338.	344.4
3000	93	322.	333.9
2500	75	307.	320.1
2000	62	293.	288.2
1500	53	283.	243.3
1000	45	273.	198.7
500	39	258.	143.0
0.0	33	-	105.0

Table B.2 Cerro Prieto M-90

Flowing Profile			Shut-in Profile	
Depth ft	Pressure psia	Temperature F	Depth ft	Temperature F
82	593.45	480.4	0.0	77
328	616.21	482.9	2292	102
656	657.44	489.0	3937	557
984	697.26	495.52	4518	567.9
1312	739.92	502.0		
1640	782.58	508.0		
1968	832.35	515.8		
2296	877.85	521.8		
2624	931.89	527.7		
2952	990.19	534.2		
3280	047.10	541.2		
3608	113.90	548.2		
3936	189.3	554.7		
4018	212.00	556.7		
4100	233.40	558.0		
4261	283.10	558.0		

Table B.3 Roosevelt Hot Springs 14-2

Flowing Profile			Shut-in Profile
Depth ft	Pressure psia	Temperature F	Temperature F
32	391		
134	403		
280	427		
554	452		
764	476		
972	500		
1177	524		
1272	536		
1378	549		
1460	561		
1539	573		
1624	585		
1694	597		
1769	609		
1880	627		
2020	652		
2116	670		
2215	688		
2301	706		
2380	724		
2450	743		
2534	761		
2580	773		
2647	791		
2715	809		
2774	827		
2832	846		
2899	864		
2955	882		
2996	894		

APPENDIX C

a) Enthalpy of liquid-gas mixture

$$h_m = \frac{H_L + H_g}{M_L + M_g} = \frac{H_L}{(M_L + M_g) M_L} M_L + \frac{H_g}{(M_L + M_g) M_g} M_g$$

$$h_m = (1 - x) \frac{H_L}{M_L} + x \frac{H_g}{M_g}$$

$$h_m = (1 - x) h_L + x h_g$$

b) Specific Volume of the mixture

$$v_m = \frac{v_L + v_g}{M_L + M_g} = \frac{v_L}{(M_L + M_g) M_L} M_L + \frac{v_g}{(M_L + M_g) M_g} M_g$$

$$v_m = (1 - x) \frac{v_L}{M_L} + x \frac{v_g}{M_g}$$

$$v_m = (1 - x) v_L + x v_g$$

c) Density of the Mixture

$$\rho_m = \frac{M_L + M_g}{v_L + v_g} = \frac{M_L}{(v_L + v_g) v_L} v_L + \frac{M_g}{(v_L + v_g) v_g} v_g$$

$$\rho_m = (1 - \alpha) \frac{M_L}{v_L} + \alpha \frac{M_g}{v_g}$$

$$\rho_m = (1 - \alpha) \rho_L + \alpha \rho_g$$